Journal of proteome research

Article

pubs.acs.org/jpr

LC–MS Proteomics Analysis of the Insulin/IGF-1-Deficient *Caenorhabditis elegans daf-2(e1370)* Mutant Reveals Extensive Restructuring of Intermediary Metabolism

Geert Depuydt,[†,§] Fang Xie,[‡,§] Vladislav A. Petyuk,[‡,§] Arne Smolders,[†] Heather M. Brewer,[‡] David G. Camp, II,[‡] Richard D. Smith,[‡] and Bart P. Braeckman*[,†]

[†]Biology Department, Ghent University, Proeftuinstraat 86 N1, B-9000 Ghent, Belgium

[‡]Biological Sciences Division and Environmental Molecular Sciences Laboratory, Pacific Northwest National Laboratory, Richland, Washington 99352, United States

Supporting Information

ABSTRACT: The insulin/IGF-1 receptor is a major known determinant of dauer formation, stress resistance, longevity, and metabolism in *Caenorhabditis elegans*. In the past, whole-genome transcript profiling was used extensively to study differential gene expression in response to reduced insulin/IGF-1 signaling, including the expression levels of metabolism-associated genes. Taking advantage of the recent developments in quantitative liquid chromatography mass spectrometry (LC–MS)-based proteomics, we profiled the proteomic changes that occur in response to activation of the DAF-16 transcription factor in the germline-less *glp-4(bn2);daf-2(e1370)* receptor mutant. Strikingly, the *daf-2* profile suggests extensive reorganization of intermediary metabolism, characterized by the upregulation of many core intermediary metabolic pathways. These include glycolysis/gluconeogenesis, glycogenesis, pentose phosphate cycle, citric acid cycle, glyoxylate shunt, fatty acid β-oxidation, one-carbon metabolism, propionate and tyrosine catabolism, and complexes I, II, III, and V of the electron transport chain. Interestingly, we found simultaneous activation of reciprocally regulated metabolic pathways, which is indicative of spatiotemporal coordination of energy metabolism and/or extensive post-translational regulation of these enzymes. This restructuring of *daf-2* metabolism is reminiscent to that of hypometabolic dauers, allowing the efficient and economical utilization of internal nutrient reserves and possibly also shunting metabolites through alternative energy-generating pathways to sustain longevity.

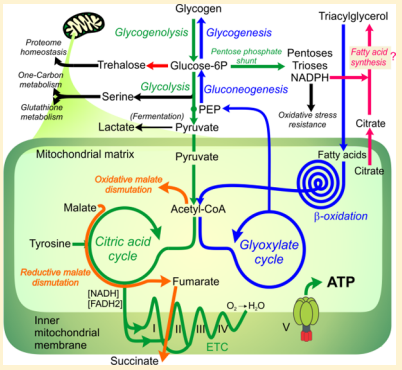

KEYWORDS: *Caenorhabditis elegans, gene expression, mass spectrometry, metabolism, physiology, aging*

INTRODUCTION

In *Caenorhabditis elegans*, attenuation of the insulin/IGF-1 signaling (IIS) pathway during adulthood leads to significant changes in worm physiology, including extended life-span, increased innate immunity and stress-resistance, and extensively altered metabolism.[1−13] These phenotypic adaptations rely, for the most part, on the activation and nuclear translocation of the forkhead box O (FOXO) transcription factor DAF-16, which triggers an extensive genetic program that is normally associated with an alternate developmental arrest state called the dauer diapause.[14−24]

In mammals, insulin signaling plays a key role in the regulation of energy metabolism.[25] Disruption of the insulin receptor in the brain is associated with expression of endocrine neuropeptides that stimulate the uptake of food, leading to obesity and symptoms of type II diabetes along with reduced reproductive competence.[26−29] In this respect, IIS in *C. elegans* appears remarkably similar to mammalian insulin signaling in that the nematode nervous system (together with the intestine) was identified as a central regulator of *daf-2*-mediated energy metabolism and longevity.[30,154] Although disruption of IIS in nematodes does not lead to any clear pathological conditions, the conservation of this pathway in the regulation of fat and carbohydrate metabolism as well as in life-span determination from nematodes to mammals is at least striking.[31−35] Therefore, a thorough understanding of *daf-2*-specific metabolism and its regulation, including species-specific peculiarities, may lead to the discovery of novel metabolic pathways involved in insulin-dependent pathologies or other fundamental processes such as aging in humans.[36,37]

Whole-genome transcript profiling of *daf-2* mutants and/or dauers, using either microarray or SAGE analysis, has proven to be successful at identifying differentially expressed gene sets dependent on DAF-16, some of which are involved in energy metabolism.[14,16−20,22,23,38,39] However, reported transcript profiles, especially with regard to energy metabolism, were sometimes inconsistent between studies, complicating the formulation of straightforward statements about IIS-mediated metabolism.[40,41] Moreover, the poor correlation between

Received: November 4, 2013
Published: February 20, 2014

mRNA transcript levels and actual protein abundances necessitates great caution when drawing conclusions based solely on interpreting transcript profiles.[42,43]

Proteomics analysis by Dong et al. of *daf-2(e1370)* mutants has identified a limited set of enzymes in carbohydrate metabolism (glycolysis/gluconeogenesis) as well as the TCA and glyoxylate cycles that are differentially expressed in *daf-2* mutants and showed that these enzymes are important determinants of nematode life span. Recently, several groups have published the first metabolite profiles of the *daf-2* mutant, revealing significant shifts in carbohydrate, amino acid, and lipid metabolism, several of which were not apparent from previously published transcriptomics studies.[11−13] Although these incentives contribute significantly to the identification of altered metabolic pathways upon impaired IIS, an integrated understanding of the metabolic restructuring and its impact on worm physiology and longevity is still lacking.

Using LC−MS/MS-based proteomics analysis, we found that activation of DAF-16 in the nucleus results in over-representation of many enzymes of major, often reciprocally regulated, metabolic pathways involved in the synthesis and utilization of internal carbohydrate (glycolysis and gluconeogenesis), lipid stores (lipogenesis and lipolysis), amino acid metabolism, and respiration (aerobic and anaerobic). In the following sections, we integrate our proteomic data set together with a selection of enzymatic activity assays, available literature, and metabolomics data in an attempt to reconstruct and resolve the intricacies of altered *daf-2* metabolism.

MATERIALS AND METHODS

C. elegans Strains

The following strains were used in this study: NLGA154 *glp-4(bn2ts)*I;*daf-2(e1370)*III (long-lived) and GA153 *glp-4(bn2ts)*I *daf-16(mgDf50)*I;*daf-2(e1370)*III (reference strain), which were kindly provided by David Gems at the University College of London.[39] The *glp-4(bn2)* background allele results in germline-deficient worms when grown at the nonpermissive temperature of 24 °C. This allows for focusing on the proteome of aging somatic cells, excluding the gonadal and complex embryonic material.[44] Previous lifespan analyses by McElwee et al. and Tekipe and Allballay demonstrated that no increase in lifespan results from the presence of the *glp-4(bn2)* allele in otherwise wild-type or *daf-16;daf-2* mutants grown on live *Escherichia coli*.[39,45] However, *glp-4(bn2)* causes a small but significant DAF-16-dependent extension of lifespan of *daf-2* mutants and nematodes grown on killed *E. coli*.[39,45] Previous MS proteome profiling of *glp-4(bn2)* after ^{15}N metabolic labeling revealed only modest changes compared to the N2 wild-type.[46] The RNAi-hypersensitive NL2099 *rrf-3(pk1426)* II strain was used for RNAi lifespan analyses.

C. elegans Culturing and Sampling

The initiation and culturing of large age-synchronized populations have been described in Depuydt et al.[47] To prevent *glp-4 daf-16;daf-2* animals from becoming dauer larvae, worms were grown at 16 °C until the third larval stage (L3) and were then shifted to 24 °C for the remainder of the experiment. Although shifting temperature at the L3 stage rendered *glp-4;daf-2* animals sterile, we noticed that by day 2 of adulthood *glp-4 daf-16;daf-2* mutants exhibited gonads with incomplete morphogenesis, yet they were able to produce 2−4 eggs per animal. Therefore, we opted to add 5-fluoro-2′-deoxyuridine (FUdR, 75 μM fc., Acros Organics) to all mass cultures in all biological replicates in order to maintain complete sterility.

We note that the use of FUdR in light of recent reports warrants caution, especially with regard to insulin/IGF-1 mutants.[155−157] However, we argue that our data reflect bona fide metabolic changes in response to the *daf-2* mutation. Our results are in line and corroborate with the reported metabolomics findings by Fuchs et al. who used both the *daf-2(e1370)* and *daf-2(m41)* alleles without the use of FUdR in their cultures.[13] Also, the *daf-2(e1370)* proteomic fingerprint made by Dong et al. in the absence of FUdR identified a limited number of differentially expressed enzymes in carbohydrate, fatty acid, and amino acid metabolism whose expression pattern was confirmed in our study. A wealth of transcriptomics data is available that show extensive changes in metabolic gene expression upon DAF-16 activation in the absence of FUdR.[13−18,23] Although there is poor concordance between these studies, our data correspond reasonably well with reported microarray profiles (but it clashes with SAGE-generated transcript profiles). We also note that the FUdR concentration used by the Davies study is very high (400 μM, compared to the more-than-sufficient 75 μM used in our study), and the dose-dependency of FUdR was not been taken into account.[157] This 400 μM concentration, in our hands, is borderline toxic for *C. elegans*.

For all experiments, samples were collected at day 2 of adulthood and freed from dead animals, debris, and bacteria through Percoll (Sigma-Aldrich) washing and flotation on a 60% w/w sucrose solution. Animals were immediately flash frozen in liquid nitrogen and stored at −80 °C.

Proteomics Data Analysis

For comparing the metabolic profile between long-lived *glp-4(bn2);daf-2(e1370)* and reference *glp-4(bn2) daf-16(mgDf50);daf-2(e1370) C. elegans* worm strains, the accurate mass and time (AMT) LC−MS proteomics data set was used, which was published earlier by our group in Depuydt et al.[47] and is freely available through PeptideAtlas[48] at http://www.peptideatlas.org/PASS/PASS00308 (see Supporting Information file 1 for details). The same criteria as in Depuydt et al.[47] were used to determine relative protein abundances, with the exception of the following proteins that included redundant peptides arising from different expression isoforms of the same gene: TPS-1, R11A5.4, W05G11.6, T22F3.3, MDH-1, H24K24.3, GPD-1,-2,-3,-4, GPI-1, and ENOL-1.

Proteomics data was visualized with MeV (MultiExperiment Viewer), part of the TM4 microarray software suite.[49,50] Pavlidis template matching (PTM)[51] was used to rank proteins conforming to an expression pattern of interest. The PTM algorithm allows a data set to be searched for proteins of which the abundance profile matches a user-defined template profile, which is based on the Pearson correlation between the template and the proteins in the data set.[51]The Kyoto Encyclopedia of Genes and Genomes (KEGG) pathway[52] and UniProt Knowledgebase[53] were used in conjunction with the process of reconstructing the *C. elegans* metabolic network. Gene set-enrichment analysis (GSEA) was used to determine whether metabolic pathways show statistically significant differential expression as described in detail in Subramanian et al.[54] In short, a ranked list of proteins is generated according to their differential abundance level between two experimental groups. An enrichment score (ES) test statistic is calculated that reflects the degree to which a defined set of proteins is overrepresented

at one of the extremes of the entire ranked list. Positive ES values correspond with enrichment for enzymes ranked to have higher expression levels in *daf-2* mutants, whereas negative ES values correspond with enrichment for enzymes ranked to have lower expression levels. Gene sets eligible for GSEA are reported with their nominal p value and false discovery rate (FDR), calculated from 1000 permutations of the experimental group labels. The nominal p value estimates the statistical significance of the ES for a single set. The FDR is the estimated probability that an enriched set represents a false positive finding. Subramanian et al. have suggested a FDR cutoff of 25% as appropriate to signify biologically significant results.[54] The GSEA-P software used for GSEA can be found at the Broad Institute's Web site http://www.broadinstitute.org/gsea/index.jsp.

Transmission Electron Microscopy (TEM)

Day 2 young adult *glp-4(bn2) daf-16(mgDf50);daf-2(e1370)* and *glp-4(bn2);daf-2(e1370) C. elegans* nematodes were fixed, and transverse sections were taken according to Fonderie et al.[55] Electron microscopy was performed using a Jeol JEM 1010 (Jeol, Tokyo, Japan) operating at 60 kV. Digitizing of images was performed using a DITABIS system (Pforzheim, Germany).

Oil Red O Staining and Quantification

Determination of relative fat content in individual worms by oil red O staining was performed according to the protocol described in O'Rourke et al.[56] Briefly, age-synchronized worms were sampled at different ages and washed in S-buffer (0.05 M K_2HPO_4, 0.05 M KH_2PO_4, and 100 mM NaCl, pH 7.4). Nematodes were fixed in MRWB-buffer (160 mM KCl, 40 mM NaCl, 14 mM Na_2EGTA, 1 mM spermidine-HCl, 0.4 mM spermine, 30 mM Na-PIPES, pH 7.4, and 0.2% β-mercaptoethanol) containing 1% paraformaldehyde (PFA) for 1 h at room temperature with gentle stirring. Fixed worms were stored at 4 °C until all samples were collected. Nematodes were then washed with S-buffer (pH 7.4) to remove PFA and incubated in 60% isopropanol for 15 min at room temperature to dehydrate. Isopropanol was removed, and samples were stained overnight in 60% oil red O stain (0.5 g/100 mL isopropanol stock solution) with gentle stirring at room temperature. After the dye was removed by washing in S-buffer containing 0.01% triton, animals were mounted and observed with a Reichert-Jung Polyvar light microscope and imaged with an Olympus Camedia C-5050 digital camera. Corel Photopaint (Corel Corporation, Ottawa, Canada) and Fiji[57] were used for image processing and analysis. In short, the red channel of RGB images was converted to 8-bit grayscale, and the resulting pixel values were inverted. A fixed threshold was set to remove remaining background artifacts. The density per worm surface was then determined by calculating the integrated density for each worm, normalized to the total worm surface.

Enzymatic Assays

Equal amounts of worms were flash frozen in liquid nitrogen and stored at −80 °C. Worms were homogenized by bead beating (glass beads 0.248−0.318 μm) in 50 mM sodium/potassium phosphate buffer, pH 7.0, at 5000 strokes/min for 30 s. CHAPS was added at a 1% final concentration to the resulting homogenate, and the mixture was bead-beated again for another 30 s. The mixture was kept on ice for 15 min and centrifuged at 20 000 rcf for 8 min at 4 °C. The supernatant was cleared by a second centrifugation step. The enzymatic activities were assayed spectrophotometrically against the appropriate blanks at 25 °C in microtiter plate wells using an Infinite M200 multiplate reader (Tecan, Männedorf, Switzerland). Isocitrate lyase, pyruvate kinase, aconitase, and phosphenolpyruvate carboxykinase activities were assayed as described previously by Castelein et al.[58] and references therein. 6-Phosphogluconic dehydrogenase activity was assayed according to the method of Bergmeyer et al.[59] following the manufacturer's instructions (Sigma no. P4553), with the exception that only half of the described concentrations were used for NADP and 6-phosphogluconate. Fumarase activity was assayed following the protocol of Racker,[60] with the exception that only 8 mM sodium malate was used (final concentration) instead of the 50 mM in Racker's work. Activity of 3-hydroxyacyl-CoA dehydrogenase, catalyzing the conversion of S-acetoacetyl-CoA to β-hydroxybutyryl-CoA with consequent NADH consumption, was monitored according to the method by Lynen et al.[61] All enzyme activities were scaled to the protein concentration of the worm extracts, estimated by the bicinchoninic acid protein assay kit (Pierce, Rockford, IL, USA).

RESULTS AND DISCUSSION

Functional annotation clustering[62,63] of the proteomics data set[47] showed a significant enrichment of proteins involved in intermediary metabolism among long-lived *glp-4(bn2);daf-2(e1370)* compared to reference *glp-4(bn2) daf-16(mgDf50);daf-2(e1370) C. elegans* worm strains (throughout the text, we will refer to both strains as *daf-2* and *daf-16;daf-2*, respectively). During culturing of the worms, FUdR was used to maintain complete sterility of the strains. Because the use of FUdR in *C. elegans* aging studies warrants caution, we discuss this issue in more detail in the Materials and Methods (*C. elegans* culturing and sampling). Table 1 shows the result of functional annotation clustering[62,63] for entries in the KEGG database category, which deals mainly with annotation of intermediary metabolism genes.[52] By searching the UniProt Protein Knowledgebase[53] and on the basis of the available literature,[19,22,23,64] we were able to reconstruct many of the

Table 1. Functional Annotation Clustering for KEGG Pathway Terms Indicates a Significant Enrichment of *daf-2*-Upregulated Proteins Involved in Intermediary Metabolism

KEGG pathway term	number of proteins	EASE score[a]
citrate cycle (TCA cycle)	14	2.6×10^{-8}
valine, leucine, and isoleucine degradation	13	2.6×10^{-6}
tyrosine metabolism	8	1.4×10^{-5}
glycolysis/gluconeogenesis	10	2.9×10^{-5}
oxidative phosphorylation	15	7.7×10^{-5}
propanoate metabolism	9	3.0×10^{-4}
pentose phosphate pathway	6	2.0×10^{-3}
pyruvate metabolism	6	3.9×10^{-3}
fatty acid metabolism	12	$3{,}9 \times 10^{-3}$
arginine and proline metabolism	6	1.3×10^{-2}
fructose and mannose metabolism	6	2.5×10^{-2}
tryptophan metabolism	8	3.0×10^{-2}
lysine degradation	8	3.3×10^{-2}
glyoxylate and dicarboxylate metabolism	3	4.1×10^{-2}

[a]EASE score is a modified Fisher's exact p value.[63]

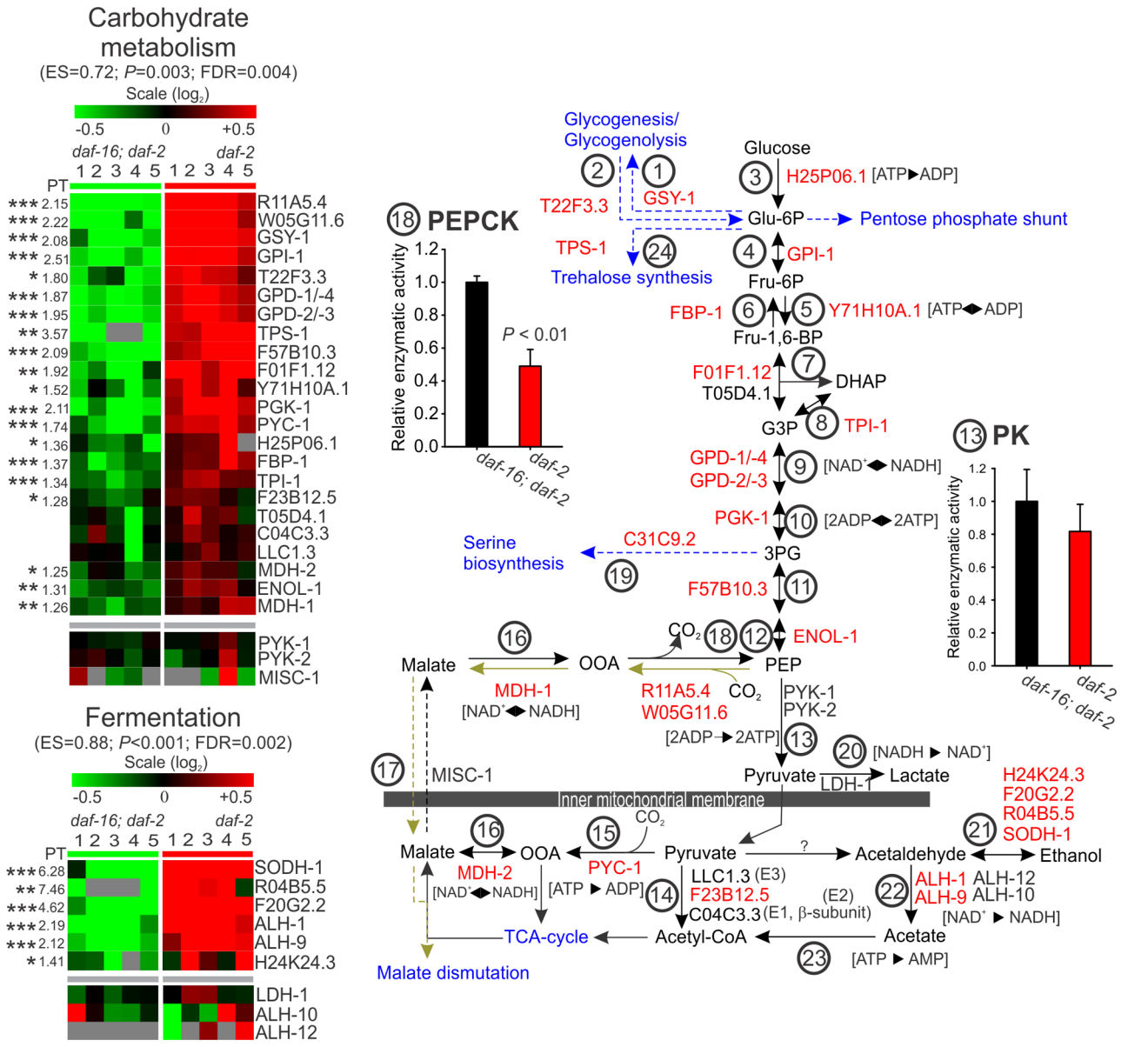

Figure 1. Carbohydrate and fermentative metabolism. (Left) Heat map of proteins that are part of carbohydrate and fermentative metabolism (base-2 logarithmic scale). Each column represents one biological replicate (five for each condition). Red and green colors indicate a relative increase and decrease in protein content for a particular protein, respectively (row). Numbers next to each heat map row denote fold change (linear) in abundance for statistically significant proteins. Proteins with significantly changed abundance levels are denoted *, $p < 0.05$; **, $p < 0.005$; and ***, $p < 0.0005$. Proteins are grouped according to whether protein profiles comply with a preset template as defined by the Pavlidis template (PT) matching algorithm (see Materials and Methods and ref 51). Green and red PT bars indicate lower and higher protein levels among strains, respectively. Gray PT bars indicate protein profiles that do not match any obvious expression pattern (see Materials and Methods for details). Gene set enrichment analysis (GSEA) allows for the assessment of whether a group of proteins (e.g., the set of genes that are part of carbohydrate metabolism in our data set) shows statistically significant differential expression as a whole (see Materials and Methods and ref 54 for more details). ES, enrichment score from gene set enrichment analysis of the metabolic pathway; p, nominal p value of the ES; FDR, false discovery rate. FDR should be ≤0.25 for the ES to be meaningful. (Right) Schematic overview of carbohydrate and fermentative metabolism. The color of protein names matches their expression profile (green, down; red, up; and black, not significant). Single-headed arrows indicate physiologically irreversible reactions. Green arrows depict the possible route of malate production via the reverse action of phosphoenolpyruvate carboxykinase and malate dehydrogenase (see Results and Discussion). Inset bar graphs represent relative enzyme activity of phosphoenolpyruvate carboxykinase (PEPCK) and pyruvate kinase (PK). (1) Glycogen synthase, (2) glycogen phosphorylase, (3) hexokinase/glucokinase, (4) phosphohexoseisomerase, (5) phosphofructokinase, (6) fructose-1,6-bisphosphate, (7) aldolse, (8) triose phosphate isomerase, (9) glyceraldehyde-3-phosphate dehydrogenase, (10) phosphoglycerate kinase, (11) phosphoglycerate mutase, (12) enolase, (13) pyruvate kinase, (14) pyruvate dehydrogenase complex (E1, pyruvate dehydrogenase; E2, dihydrolipyl transacetylase; and E3, dihydrolipoyl dehydrogenase), (15) pyruvate carboxylase, (16) mitochondrial/ cytosolic malate dehydrogenase, (17) malate-α-ketoglutarate antiporter (malate shuttle), (18) phosphoenolpyruvate carboxykinase, (19) phosphoglycerate dehydrogenase, (20) lactate dehydrogenase, (21) alcohol dehydrogenase, (22) aldehyde dehydrogenase, (23) acetyl-CoA synthetase, and (24) trehalose-6-phosphate synthase. Glu-6P, glucose-6-phosphate; Fru-6P, fructose-6-phosphate; Fru-1,6-BP, fructose 1,6-bisphosphate; DHAP, dihydroxyacetone phosphate; G3P, glyceraldehyde-3-phosphate; 3PG, 3-phosphoglycerate; PEP, phosphoenolpyruvate; and OOA, oxaloacetate.

dx.doi.org/10.1021/pr401081b | J. Proteome Res. 2014, 13, 1938−1956

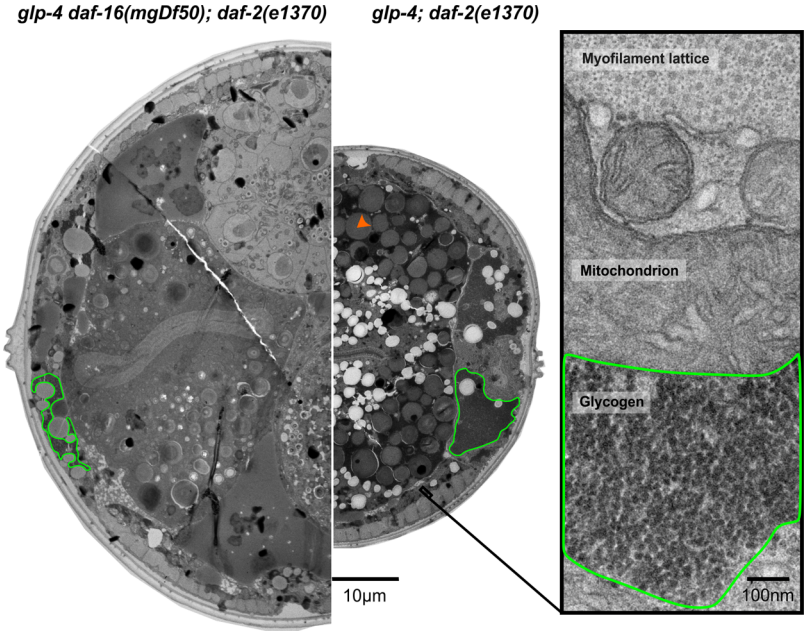

Figure 2. Transmission electron microscopy images of transversal midbody cross sections of day 2 adult nematodes. (Left) *daf-2* mutants exhibit relatively large amounts of glycogen (delineated in green) and fat droplets (orange arrowhead) stored inside hypodermal and intestinal cells compared to the reference strain. *daf-2* mutants also show a smaller cross-sectional diameter compared to the *daf-16*;*daf-2* reference. Quantitative determination of worm length, diameter, and volume of both *daf-2* and *daf-2*;*daf-16* worms is shown in Supporting Information file 2. (Right) High-magnification image (×25 000) of a small section of *daf-2* striated muscle tissue showing the tight organization of glycogen and mitochondria close to the myofilament lattice.

pathways in *C. elegans* intermediary metabolism from our data set, which is the focus of this article.

Increased Expression of Most Carbohydrate Metabolism Enzymes in *daf-2*

We detected increased protein abundance of many glycolytic enzymes in *daf-2* mutants, including hexokinase (H25P06.1) and phosphofructokinase (Y71H10A.1), two major regulatory sites of glycolysis that catalyze irreversible reactions (Figure 1). The only exception occurs in the final (irreversible) step in glycolysis catalyzed by the pyruvate kinase enzymes PYK-1 and PYK-2, which remain unaltered in *daf-2* mutants. We also find increased protein expression of enzymes in gluconeogenesis: fructose-1,6-bisphosphatase (FBP-1), pyruvate carboxylase (PYC-1), and two isoforms of phosphoenolpyruvate carboxykinase (PEPCK), R11A5.4 and W05G11.6. PEPCK constitutes a key activator of gluconeogenesis,[65] and elevated levels of PEPCK in *daf-2* mutants confirm earlier reports on PEPCK transcript and protein levels in insulin/IGF-1 signaling-defective mutants.[66,67] Simultaneous activation of glycolysis and gluconeogenesis would lead to a futile cycle, generating heat at the cost of ATP hydrolysis. This seems unlikely because *daf-2* mutants have lower mass-specific thermogenesis and both pathways are reciprocally regulated.[64,68] To investigate the relative activities of glycolysis/gluconeogenesis, we measured in vitro enzymatic activities of PEPCK (gluconeogenesis) and pyruvate kinase (glycolysis) (Figure 1). Surprisingly, in stark contrast with the more than doubled PEPCK enzyme levels, relative PEPCK enzymatic activity in *daf-2* mutants was only 50% compared to the *daf-2*;*daf-16* reference, indicating that gluconeogenesis in young adult *daf-2* mutants is repressed. In contrast, pyruvate kinase activity remains unchanged in the *daf-2* mutant, suggesting normal glycolysis activity.

We also found significantly elevated protein levels of both glycogen synthase-1 (GSY-1/Y46G5A.31, glycogenesis) and the orthologue of human glycogen phosphorylase (T22F3.3, catalyzing the first step in glycogenolysis) in *daf-2* adults (Figure 1). Ultrastructural and biochemical studies showed *daf-2* mutants and dauers store significantly more glycogen in their intestinal and hypodermal cells compared to wild-type nematodes.[69,70] Electron micrographs taken from our samples also confirmed the presence of high amounts of glycogen in hypodermal cells and body-wall muscles of *daf-2* mutants (Figure 2), consistent with increased glycogen synthase activity. The fermentation of stored glycogen constitutes a major source of energy during anoxia/hypoxia and is determinate for nematode survival under these conditions.[69,71] Consistently, the increased survival of *daf-2* mutants during anoxic insult is dependent on its high glycogen levels.[8,69] In addition, in dauer larvae, high glycogen reserves likely serve to maintain their high degree of motility during the first few weeks after dauer formation,[72] which is in agreement with the expression of glycogen phosphorylase in *C. elegans* muscles.[73]

We found significantly increased protein levels of TPS-1, one of two *C. elegans* trehalose-6-phosphate synthase genes responsible for trehalose biosynthesis, consistent with increased trehalose levels in IIS-defective *C. elegans* mutants and dauers[13,74,75] and DAF-16-dependent transcription regulation.[16,17,76] Importantly, *tps-1* and *tps-2* were found to be required, in part, for *daf-2* longevity.[74] Besides its role in carbohydrate storage and transport,[77,78] trehalose also has extensive cytoprotective functions, most probably by stabilizing the proteome and lipid membranes under various stress conditions, including cold, heat, dehydration, hypoxic, and oxidative insult.[79−81] Elevated levels of trehalose are associated with life-span extension in *C. elegans*[74] and also render *daf-2* dauers resistant to extreme desiccation.[81]

dx.doi.org/10.1021/pr401081b | *J. Proteome Res.* 2014, 13, 1938−1956

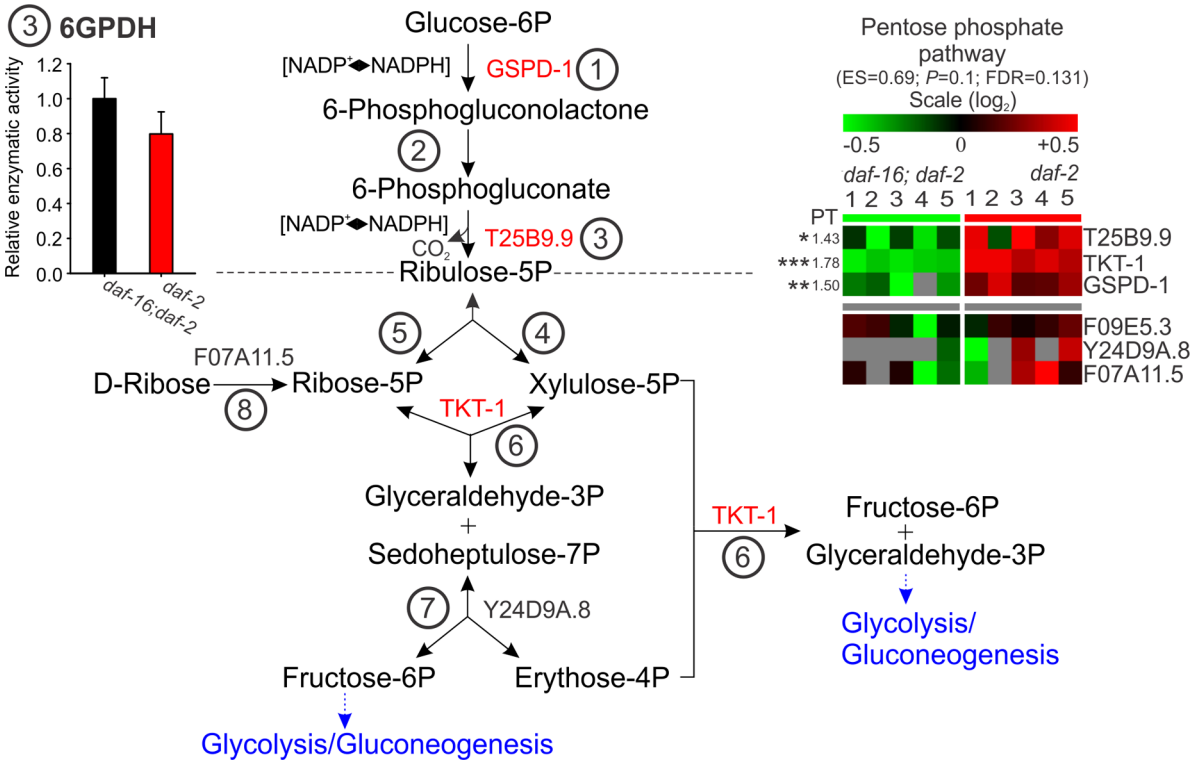

Figure 3. Pentose phosphate pathway. (Right) Heat map (base-2 logarithmic scale) and (left) schematic overview of proteins that are part of the pentose phosphate pathway. Numbers next to each heat map row denote fold change (linear) in abundance for statistically significant proteins. Proteins with significantly changed abundance levels are denoted *, $p < 0.05$; **, $p < 0.005$; ***, $p < 0.0005$. (1) Glucose-6-phosphate degydrogenase, (2) gluconolactone hydrolase, (3) 6-phosphogluconate dehydrogenase, (4) ribulose-5-phosphate-3-epimerase, (5) ribose-5-phosphate-ketoisomerase, (6) transketolase, (7) transaldolase, and (8) ribokinase. Inset bar graph represents relative enzyme activity of 6-phosphogluconate dehydrogenase (6PGDH).

Pentose Phosphate Pathway Enzymes Are Upregulated in *daf-2*

Our data show a significant upregulation in the expression of three enzymes predicted to be part of the pentose phosphate pathway, including GSPD-1, the *C. elegans* orthologue of glucose-6-phosphate dehydrogenase (G6PDH), which catalyzes the first step in the pentose phosphate pathway and converts $NADP^+$ into NADPH (Figure 3). However, we found no significant difference in the activity of this pathway by measuring the enzymatic activity of 6-phosphogluconate dehydrogenase (Figure 3). Nonetheless, temporal activation of this pathway could be involved in the increased oxidative stress resistance of the *daf-2* mutant because the rerouting of carbohydrate intermediates from glycolysis to the pentose phosphate shunt has been shown to be part of a coordinated response to oxidative stress by maintaining high cytoplasmatic $NADPH/NADP^+$ ratios in *C. elegans*, *Drosophila*, and mammals.[82−86]

Activation of Alcohol Fermenting Enzymes in *daf-2*

A strong upregulation was found of several putative alcohol dehydrogenases and aldehyde dehydrogenases involved in alcohol metabolism (Figure 1). Alcohol dehydrogenases include the predicted sorbitol dehydrogenases SODH-1 and its homologue R04B5.5, the ribitol-dehydrogenase domain containing protein F20G2.2.[19,87] The actual substrate of these alcohol dehydrogenases is unknown at present, but *sodh-1* appears capable of metabolizing ethanol.[88] SODH-1 is known to be activated by DAF-16,[17,19,89] and higher mRNA levels of *sodh-1* were also found in long-lived worms cultured axenically.[58] Furthermore, SODH-1 was the most upregulated (1200%) spot in 2D-DIGE gels from *Staphylococcus aureus*-treated worms but not in *Aeromonas hydrophila*-treated worms.[90,91] Therefore, the biological role of this enzyme may reach further than fermentative metabolism. Indeed, some alcohol dehydrogenase enzymes are also capable of neutralizing cytotoxic aldehydes originating from lipid peroxidation, including 4-hydroxynonenal (4-HNE).[92,93]

ALH-1 is an orthologue of mitochondrial aldehyde dehydrogenase 2 in humans that possibly catalyzes the conversion of acetaldehyde, resulting from the oxidation of ethanol, into acetate. Although we found strongly increased abundance of ALH-1 in *daf-2* mutants, metabolomic profiles of *daf-2* mutants indicate a significant drop in acetate content in IIS mutants.[13] ALH-1 is also involved in the detoxification of toxic aldehyde byproducts of alcohol metabolism or lipid peroxidation.[94,95] More specifically, *C. elegans* ALH-1 was shown capable to oxidize 4-HNE further to the lesser reactive 4-HNA (4-hydroxynon-2-enoic acid), similar to mammalian aldehyde dehydrogenase.[96] On the basis of these reports, the activation of alcohol-fermenting enzymes in *daf-2* mutants may well be part of a coordinated stress response system that boosts the nematodes resistance to toxic byproducts of lipid and intrinsic alcohol metabolism.

Most Citric Acid Cycle Enzymes Are Upregulated in *daf-2* Mutants

A general increase was found of the citric acid cycle enzymes, including citrate synthase, the isocitrate dehydrogenase complex, and the α-ketoglutarate dehydrogenase complex,

dx.doi.org/10.1021/pr401081b | J. Proteome Res. 2014, 13, 1938−1956

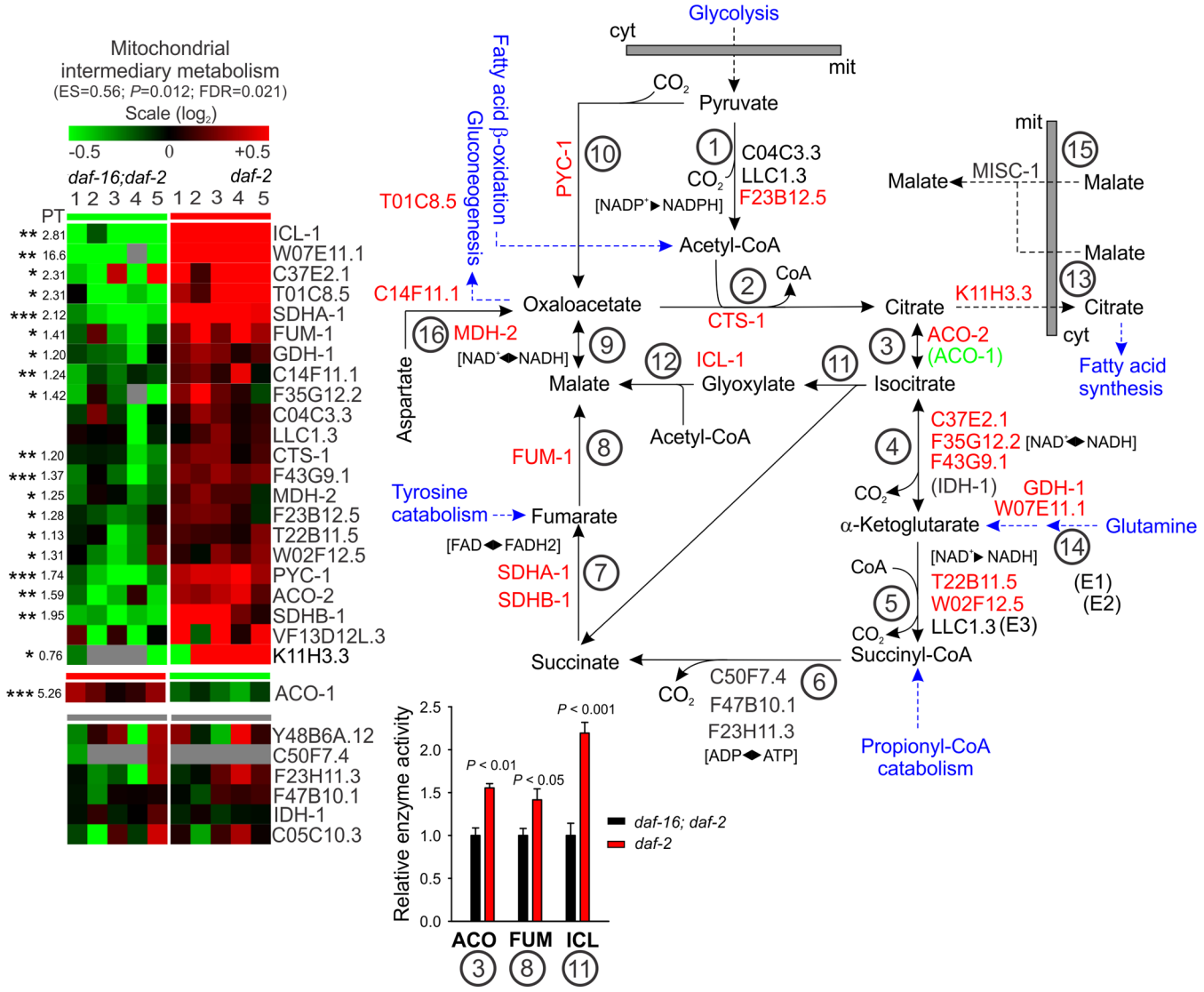

Figure 4. Mitochondrial intermediary metabolism. (Left) Heat map (base-2 logarithmic scale) and (right) schematic overview of enzymes in mitochondrial intermediary metabolism. Numbers next to each heat map row denote fold change (linear) in abundance for statistically significant proteins. Proteins with significantly changed abundance levels are denoted *, $p < 0.05$; **, $p < 0.005$; and ***, $p < 0.0005$. Inset bar graphs represent relative enzymatic activities of aconitase, fumarase, and isocitrate lyase. (1) Pyruvate dehydrogenase complex, (2) citrate synthase, (3) aconitase, (4) isocitrate dehydrogenase complex, (5) α-ketoglutarate dehydrogenase complex (E1, oxoglutarate dehydrogenase; E2, dihydrolipoyl succinyl transferase; and E3, dihydrolipoyl dehydrogenase), (6) succinate thiokinase, (7) succinate dehydrogenase, (8) fumarase, (9) malate dehydrogenase, (10) pyruvate carboxylase, (11) isocitrate lyase, (12) malate synthase, (13) mitochondrial tri/dicarboxylate carrier protein, (14) GDH-1, glutamate dehydrogenase; W07E11.1, glutamate synthase, (15) malate-α-ketoglutarate antiporter (malate shuttle), and (16) aspartate aminotransferase. Succ, succinate; succ-CoA, succinyl-CoA; ACO, aconitase; and FUM, fumarase.

which was the main sites of regulation within this cycle (Figure 4). This increase is accompanied with higher activity of fumarase and aconitase in vitro (Figure 4). Transcript profiles of *daf-2* mutants did not show any significant change in mRNA levels for citric acid cycle enzymes.[23,24] Expression of these genes therefore may be regulated post-transcriptionally or be the result of lowered turnover of these enzymes or the mitochondria in which they reside. Here, *daf-2* energy metabolism appears to differ from that of the dauer larva, which is characterized by both reduced gene expression and enzymatic activity of citric acid cycle genes.[22,97,98] We note that the aconitase, ACO-1, is downregulated in *daf-2* mutants. However, ACO-1 is thought to be a cytosolic aconitase involved in the regulation of cellular iron concentrations and is therefore not part of the citric acid cycle.[99] Similarly, IDH-1 is a predicted cytosolic NADP-dependent isocitrate dehydrogenase (IDH) and shows no upregulation in *daf-2*.[23] We note here that cytosolic NADP-dependent IDH activity is strongly increased in the *daf-2* mutant (data not shown).

daf-2 Glyoxylate Shunt Is Activated, as in Dauers

The glyoxylate shunt allows the synthesis of carbohydrates via gluconeogenesis from acetyl-CoA obtained from fatty acid β-oxidation and is generally known in plant and microorganism biochemistry. Nematodes also have been shown to contain an active glyoxylate shunt,[100,101] which is required for the full longevity phenotype of *daf-2* and several ETC-defective mutants (Mit mutants) as well as the mitochondrial mutant *clk-1(qm30)*.[17,102,103] In *C. elegans*, the key glyoxylate cycle enzymes, isocitrate lyase and malate synthase, are contained as two separate structural domains in a single protein, ICL-1.[104]

dx.doi.org/10.1021/pr401081b | J. Proteome Res. 2014, 13, 1938−1956

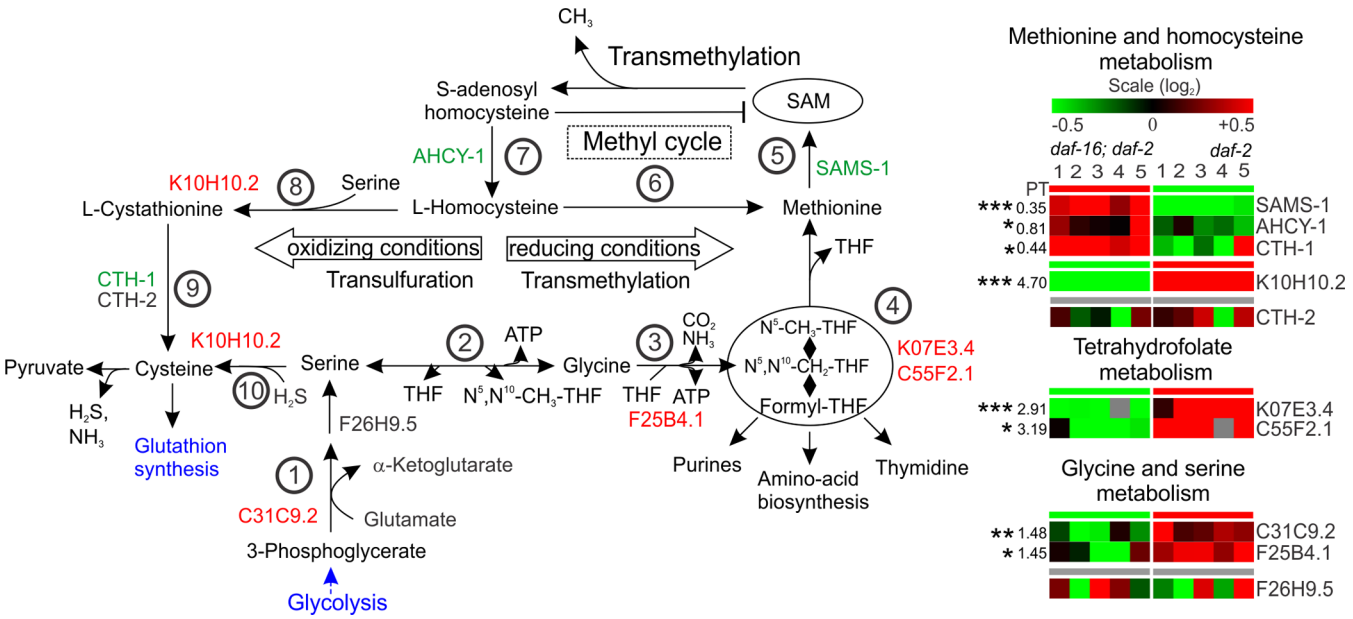

Figure 5. One-carbon pool metabolism. (Right) Heat map (base-2 logarithmic scale) of enzymes part of *C. elegans* one-carbon metabolism. (Left) Shematic overview of one-carbon metabolism involving both the single-carbon carriers tetrahydrofolate and S-adenosylmethionine. Numbers next to each heat map row denote fold change (linear) in abundance for statistically significant proteins. Proteins with significantly changed abundance levels are denoted *, $p < 0.05$; **, $p < 0.005$; and *** $p < 0.0005$. (1) Phosphoglycerate dehydrogenase (C31C9.2), phosphoserine aminotransferase (F26H9.6), (2) serine hydroxymethyl transferase, (3) glycine cleavage system T-protein (aminomethyltransferase), (4) AICAR formyltransferase (C55F2.1), C1-THF-synthase (K07E3.4), (5) S-adenosyl methionine synthase, (6) methionine synthase, (7) S-adenosylhomocysteinase, (8 and 10) cystathionine β-synthase/cysteine synthase, and (9) cystathionine γ-lyase. THF, tetrahydrofolate.

We observed a very strong increase in ICL-1 abundance, consistent with previous transcriptional evidence.[17,22,23] Consistently, in vitro activity of both isocitrate lyase and malate synthase is increased in *daf-2* (Figure 4) and *age-1*[98] mutants, respectively.

Major Shift in One-Carbon Metabolism in *daf-2*

One-carbon metabolism involves the storage and utilization of one-carbon moieties in anabolic and transmethylation-based regulatory pathways.[105] The carrier of activated one-carbon fragments is tetrahydrofolate (THF), an essential water-soluble derivative of vitamin B9 involved in the formation of nucleotides for DNA synthesis, the metabolism of certain amino acids, and the source of methyl groups for S-adenosyl methionine (SAM).[106] A particularly strong increase was found in the protein levels of the putative *C. elegans* AICAR formyltransferase (C55F2.1) and C1-THF synthase (K07E3.4) in *daf-2*, both of which are involved in the interconversion of one-carbon derivates of THF (Figure 5). Serine is the major donor of one-carbon in the form of N^5,N^{10}-CH_2-THF through its catabolism via glycine.[107] We found increased levels in the *daf-2* mutant of phosphoglycerate dehydrogenase (C31C9.2), which catalyzes the first step in glucose-derived serine biosynthesis, and F25B4.1, the *C. elegans* orthologue of the glycine cleavage system T-protein, an aminomethyltransferase that catalyzes the actual transfer of methylene carbon from the decarboxylated glycine to tetrahydrofolate (THF). Taken together, our results suggest changes in THF-based anabolism in *daf-2* mutants, possibly fueled via de novo synthesis of serine and subsequent oxidation over glycine to supply one-carbon units.

In contrast to THF-metabolism, the biosynthetic pathway of SAM, the other main carrier for single-carbon units, appears repressed in *daf-2* mutants (Figure 5). S-adenosylmethionine synthase activity produces SAM by catalyzing the condensation of methionine with ATP. Protein levels of this enzyme (SAMS-1) are strongly reduced in the *daf-2* mutant. Demethylation of SAM results in the production of S-adenosylhomocysteine (SAH), which is a strong inhibitor of all SAM-dependent transmethylation reactions.[108] S-adenosylhomocysteinase catalyzes the hydrolytic cleavage of SAH into homocysteine plus adenosine, but expression of this enzyme (AHCY-1) at the protein level also appears significantly reduced in *daf-2* mutants. Homocysteine lies at the cross-point of two competing pathways: it is either used to form methionine (for SAM synthesis) via the remethylation pathway or to form cysteine via the transsulfuration pathway.[108] Transsulfuration of homocysteine to cysteine is catalyzed by two enzymes: cystathione β-synthase (CBS), which forms cystathionine from homocysteine and serine, and cystathionine γ-lyase, which converts cystathionine to cysteine, α-ketobutyrate, and ammonia. The putative *C. elegans* orthologue of CBS (K10H10.2) is strongly upregulated in *daf-2*, suggesting increased funneling of homocysteine toward cysteine synthesis, away from remethylation of homocysteine into methionine. Because cysteine is normally readily available from diet, the major role of the transsulfuration pathway in animals is thought to be the regulation of SAM levels by controlling methionine/homocysteine degradation and not cysteine biosynthesis per se.[109] Thus, high CBS activity in *daf-2* mutants is an additional strong indication of repressed SAM synthesis. In contrast, the putative *C. elegans* cystathionine γ-lyase orthologue CTH-1 is downregulated, and its paralogue, CTH-2, shows no change in expression. Because there is no apparent alternate route for the further processing of cystathionine, it seems that reduced CTH-1 expression aims to temper the increased flux through CBS. Taken together, our data strongly suggest a reduced flux through the methyl cycle in *daf-2* mutants.

dx.doi.org/10.1021/pr401081b | J. Proteome Res. 2014, 13, 1938−1956

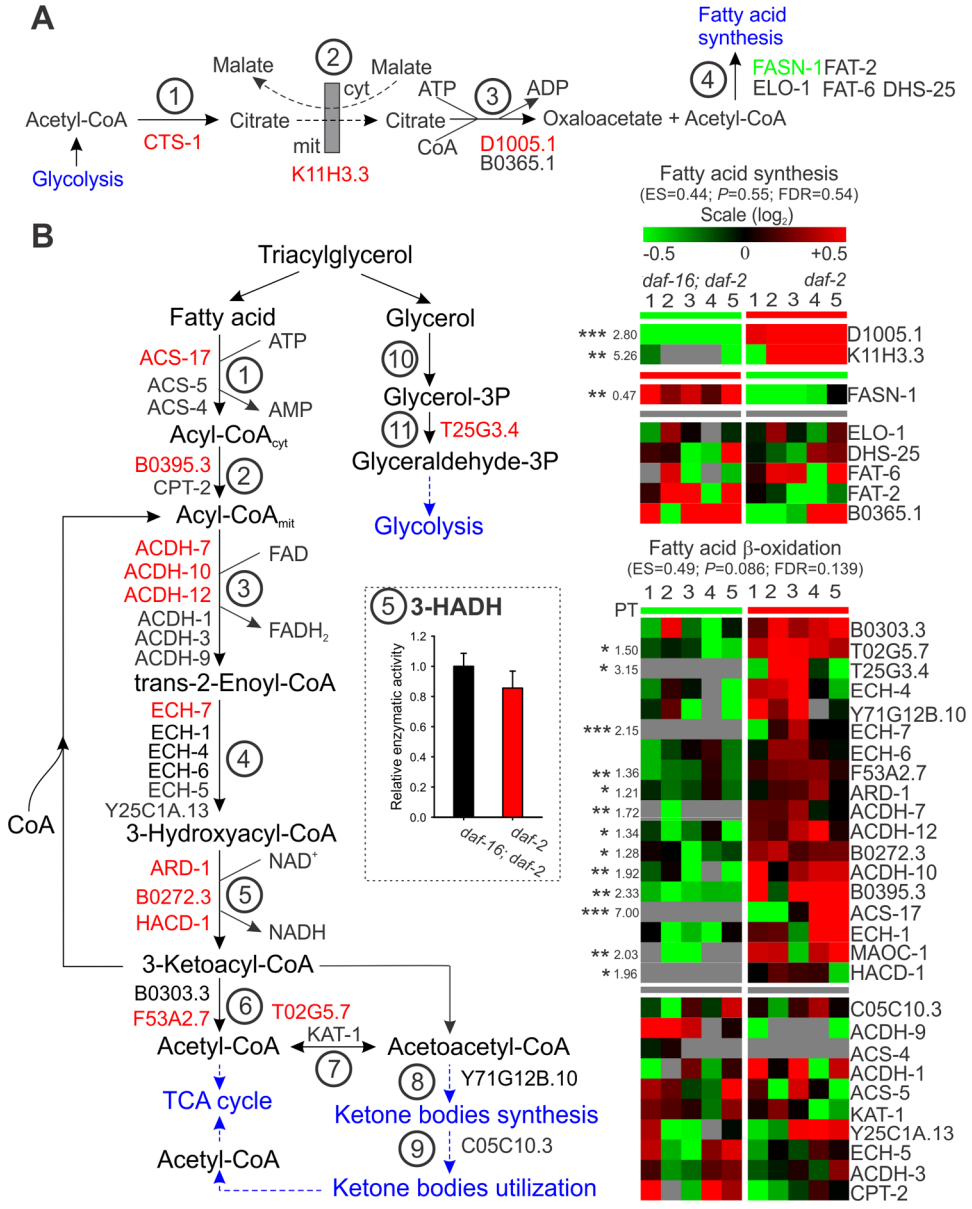

Figure 6. Fatty acid metabolism. (A) Synthesis of fatty acids. (Right) Heat map and (left) schematic overview of enzymes implicated in fatty acid synthesis. (1) Citrate synthase, (2) mitochondrial tricarboxylate/dicarboxylate carrier protein (citrate transport protein), (3) ATP-citrate lyase, and (4) FASN-1, fatty acid synthase; ELO-1, long-chain fatty acid elongase; DHS-25, mitochondrial beta-ketoacyl-ACP reductase; FAT-6 and FAT-2 encode fatty acyl desaturases. 3-HADH, 3-hydroxyacyl-CoA dehydrogenase. (B) Oxidation of fatty acids. (Right) Heat map and (left) schematic overview of detected fatty acid β-oxidation enzymes. Numbers next to each heat map row denote fold change (linear) in abundance for statistically significant proteins. Proteins with significantly changed abundance levels are denoted *, $p < 0.05$; **, $p < 0.005$; and ***, $p < 0.0005$. Inset bar graph represent relative enzymatic activity of acyl-CoA dehydrogenase. (1) Acyl-CoA synthetase, (2) carnitine O-acyltransferase, (3) acyl-CoA dehydrogenase, (4) trans-2-enoyl-CoA hydratase, (5) 3-hydroxyacyl-CoA dehydrogenase, (6) thiolase, (7) acetyl-CoA acetyltransferase (thiolase), (8) 3-hydroxy-3-methylglutaryl-CoA (HMG-CoA) lyase, and (9) succinyl-CoA-acetoacetate CoA transferase.

Adult *daf-2* Mutants Show Increased Reliance on Internal Fat Stores

In mammals, fatty acid synthesis is initiated by citrate transport across the mitochondrial membranes into the cytoplasm via tricarboxylate carriers (TIC) in exchange with malate.[110] Once in the cytosplasm, citrate is cleaved by ATP-citrate lyase (ACL) into acetyl-CoA and oxaloacetate.[111] This enzyme is the main source for cytosolic acetyl-CoA for fatty acid synthesis and represents a major link between the citric acid cycle and lipogenesis.[111] In mammals, expression of this mitochondrial citrate carrier is activated by insulin signaling,[110,112] and inhibition of ACL was shown to reduce fatty acid synthesis significantly and to increase fatty acid β-oxidation.[113] We found strongly increased abundance of the *C. elegans* mitochondrial TIC (K11H3.3) and ACL (D1005.1) in *daf-2* mutants compared to the reference strain, suggesting increased lipogenesis (Figure 6B). Paradoxically, we found a strong suppression of the predicted *C. elegans* fatty acid synthase, FASN-1, in *daf-2* adults. This suggests that in adult *daf-2* worms fatty acid synthesis is attenuated even in the presence of plenty of substrates. We note that the *C. elegans* genome contains at least three other putative fatty acid synthase genes (C41A3.1, F10G8.9, and F32H2.6), which could also be important determinants of fatty acid synthesis.

dx.doi.org/10.1021/pr401081b | J. Proteome Res. 2014, 13, 1938−1956

At the same time, we found increased expression in *daf-2* adults of many fatty acid β-oxidation proteins (Figure 6A) as well as an enzyme involved in glycerol catabolism (T24G3.4) and a choline/carnitine palmitoyl transferase (B0395.3). The latter is possibly responsible for the translocation of long-chain fatty acids into the mitochondrial matrix prior to oxidation. We also found increased protein levels of MAOC-1, a predicted peroxisomal fatty acid β-oxidase enzyme. To assess whether fatty acid β-oxidation is increased in the *daf-2* mutant, we measured the in vitro activity of 3-hydroxyacyl CoA dehydrogenase, which catalyzes the oxidation of L-3-hydroxyacyl CoA, and found that its activity was unchanged (Figure 6). Nonetheless, the coordinated upregulation of most β-oxidation enzymes clearly indicates that *daf-2(e1370)* worms tend to rely more on internal fat stores compared to wild type to fuel their energy needs. The formed acetyl-CoA is either further oxidized to CO_2 and water in the citric acid cycle or, alternatively, acetyl-CoA is converted into succinate and malate via the upregulated glyoxylate cycle for use in gluconeogenesis. In addition, glyceraldehyde-3-phosphate derived from the catabolism of glycerol can be fed into the glycolytic pathway for energy generation. We note that the relative increase in β-oxidation proteins found in our study appears not to be reflected at the transcript level, as both SAGE- and microarray-based transcript profiling detected no change in the mRNA expression of β-oxidation enzymes in *daf-2* mutants.[18,23]

On the basis of our results, we hypothesize that *daf-2* mutants switch from fat synthesis and storage during development and early adulthood to controlled lipid breakdown for the remainder of life, mimicking the dauer larva.[114] To test this hypothesis, we determined the age-dependent alterations in fat content of *daf-2* mutants and *daf16;daf-2* reference worms by staining with the fat-soluble dye oil red O (Figure 7).[56] We combined these results with data on the feeding behavior of the same IIS mutants (but lacking the *glp-4* mutation) collected over many aging series that were run independently in liquid cultures in our lab. As expected, our data show that *daf-2* mutants accumulate significantly more fat than the *daf-16;daf-2* reference at day 2 of young adulthood. Although we noticed a sudden drop in oil red O intensity at day 6 of adulthood, *daf-2* mutants were able to maintain relatively high fat content, whereas in reference worms, fat levels decreased steadily with age. This result is remarkable given that *daf-2(e1370)* mutants exhibit a clear Eat phenotype (reduced food uptake) that manifests itself during early adulthood (Figure 7). Therefore, *daf-2* fat metabolism is reminiscent to the nonfeeding dauer larva, which depends on the slow and controlled release of energy and anabolic intermediates via β-oxidation of internal fat stores for its survival.[22,72,114−116]

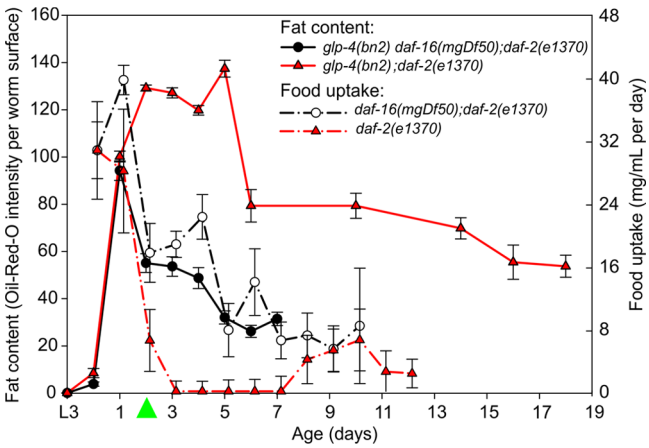

Figure 7. Age-related change in fat content and feeding behavior. Nematodes were stained with oil red O to determine the relative fat content in individual worms. For each time point, between 10 and 22 nematodes were analyzed per strain. The amount of *E. coli* in grams required each day to maintain a constant turbidity (OD_{550} = 1.8) in culture medium (liquid cultures) was used as a measure to assess the feeding behavior as a function of age. We note that zero values for oil red O intensity do not indicate that these animals are devoid of fat but merely indicate the detection limit of this dye for quantifying fat levels. Green arrowhead represents time of sampling for proteomics analysis.

daf-2 Mutants May Catabolize Their High Propionate Levels

The *daf-2* mutant has been shown to contain increased levels of propionate.[13] The carbon atoms of propionate are recycled into the citric acid cycle component succinyl-CoA via an evolutionary conserved multienzyme pathway that was shown to be fully functional in *C. elegans* (Figure 8).[117,118] We detected significantly increased abundance of the propionate catabolic enzymes methylmalonyl-CoA racemase (MCE-1), methylmalonyl-CoA mutase (MMCM-1), and the alpha (PCCA-1) and beta (PCCB-1) subunits of propionyl-CoA decarboxylase in *daf-2* adult animals (Figure 8).

Propionate is either activated to propionyl-CoA by an appropriate acyl-CoA synthetase or originates directly from the catabolism of the branched amino acids valine and isoleucine or β-oxidation of odd-chain-length fatty acids.[64] Activation of this catabolic pathway would thus indicate increased catabolism of fatty acids or branched chain amino acids in the *daf-2* mutant.

Amino Acid Catabolism May Replenish the TCA Cycle in the *daf-2* Mutant

Recent metabolomic profiling studies of the *daf-2* mutant have revealed an increase in the concentration of free amino acids, in particular of branched-chain amino acids (BCAAs), suggesting altered amino acid metabolism in this mutant.[12,13] In accordance, we report an increase in the level of glutamate dehydrogenase (GDH-1), an enzyme essential in amino acid breakdown that catalyzes the deamination of glutamate into α-ketoglutarate (Figure 4). We also find a dramatic increase (16.6-fold) in the putative glutamate synthase W07E11.1, which catalyzes the formation of glutamate from glutamine. In mammals, glutamine serves as a universal transporter of nitrogen and is the most common free amino acid in human blood plasma. Interestingly, Martin et al. showed that the level of glutamine and glutamate were increased and decreased, respectively, in the *daf-2* mutant.[12] We speculate that the strong increase of glutamate synthase in combination with glutamate dehydrogenase is indicative of increased amino acid catabolism in the *daf-2* mutant, fueling the TCA cycle.

Also consistent with increased amino acid catabolism is the clear increase of most tyrosine catabolic enzymes, including HPD-1 (Figure 9a).[119] Our result is consistent with an earlier proteomics report where fumarylacetoacetate hydrolase (K10C2.4) was found to be significantly upregulated in the *daf-2* mutant.[67] Moreover, the transcript level of cytosolic tyrosine aminotransferase (TAT, F24D1.2), which catalyzes the first step in tyrosine catabolism, was found to be highly enriched in dauers.[19]

dx.doi.org/10.1021/pr401081b | J. Proteome Res. 2014, 13, 1938−1956

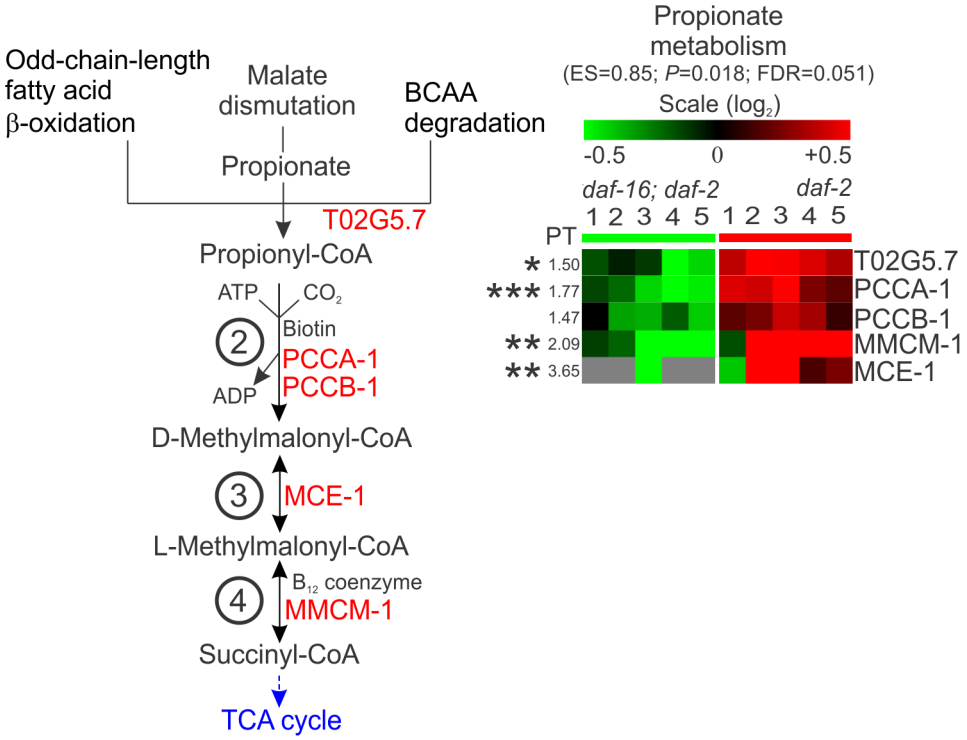

Figure 8. Propionate metabolism. (Right) Heat map and (left) schematic overview of propionate metabolism enzymes. Numbers next to each heat map row denote fold change (linear) in abundance for statistically significant proteins. Proteins with significantly changed abundance levels are denoted *, $p < 0.05$; **, $p < 0.005$; and ***, $p < 0.0005$. (2) Propionyl-CoA carboxylase, (3) methylmalonyl-CoA racemase, and (4) methylmalonyl-CoA isomerase.

The level of cellular tyrosine is thought to be determined by insulin signaling through modulation of tyrosine catabolism.[19,120] Like in mammals, *C. elegans* TAT and the gluconeogenic enzyme PEPCK both contain an insulin-responsive element (IRE) in the promoter region, conferring insulin-induced inhibition of expression. Thus, rather surprisingly and in contrast with our and others proteome data,[67] reduced insulin signaling in *C. elegans* has been associated with the transcriptional repression of tyrosine catabolic enzyme *hpd-1*.[15] This discrepancy between transcript and protein levels indicates complex regulation of tyrosine catabolism enzymes.

In contrast to tyrosine, we found reduced concentrations of BCAA catabolic enzymes, including the branched-chain aminotransferase enzyme (BCAT-1), in the *daf-2* mutant (Figure 9b), in line with transcriptional evidence and paralleled by increased levels of BCAAs as reported previously by us[47] and others.[12,13]

Finally, we also found increased abundance of the aspartate aminotransferases T01C8.5 and C14F11.1 (Figure 4), which catalyze the interconversion of aspartate and α-ketoglutarate into oxaloacetate and glutamate.

Complexes of the *daf-2* Electron Transport Chain Are Differentially Regulated

An increased protein level of several subunits of complexes I and II and to a lesser extent complexes III and V was found in *daf-2* mutants (Figure 10). Remarkably, protein expression of cytochrome C oxidase (complex IV) was repressed in *daf-2*. Cytochrome C oxidase catalyzes the terminal reduction of one O_2 molecule to two molecules of H_2O with the additional translocation of four protons to the intermembrane space. If complex IV activity is reduced in *daf-2* animals, then it can be expected that less oxygen is consumed compared to wild type. A slightly reduced mass-specific metabolic rate, as measured by carbon dioxide gas respirometry, has been reported in *daf-2* mutants.[121] However, no decrease in oxygen consumption between *daf-2(e1370)* and wild-type or *daf-16(m26);daf-2(e1370)* has been observed in locomotory active worms.[10,68,122] Carbon dioxide gas respirometry is expected to leave the worms practically undisturbed on a spot of *E. coli* bacteria,[121] whereas direct oxygen consumption measurements in liquid require extensive stirring, stimulating worm movement and thus metabolic activity, which could explain the discrepancy in reported *daf-2(e1370)* metabolic rates.[10] In addition, adult *daf-2* mutants cultured on undisturbed agar plates appear to be rather inactive when compared to the reference strain,[123,124] but they retain the ability to move freely in response to, for example, mechanical stimulation, similar to dauers.[125] *daf-2* mutants are also characterized by reduced food uptake (as was discussed earlier) and low heat output.[10] Therefore, we suggest that *daf-2* standard metabolism, like dauers, is hypometabolic, but the metabolic rate is readily raised when necessary, and this is ensured by the availability of large amounts of fat and glycogen and the increased levels of enzymes of core intermediary metabolism.

We also found elevated protein levels of the electron-transferring flavoproteins (ETF) F27D4.1 and ETF-dehydrogenase (LET-721) in *daf-2* mutants, although the latter upregulation was not statistically significant. These proteins transfer the electron pair of $FADH_2$, resulting from the β-oxidation of acyl-CoA, to the flavo-iron–sulfur protein ETF-dehydrogenase, which in turn reduces coenzyme Q in the electron transport chain in the mitochondrial inner membrane.[126] This is in line with the enhanced fatty acid oxidation pathway in *daf-2* mutants, as described above.

dx.doi.org/10.1021/pr401081b | J. Proteome Res. 2014, 13, 1938−1956

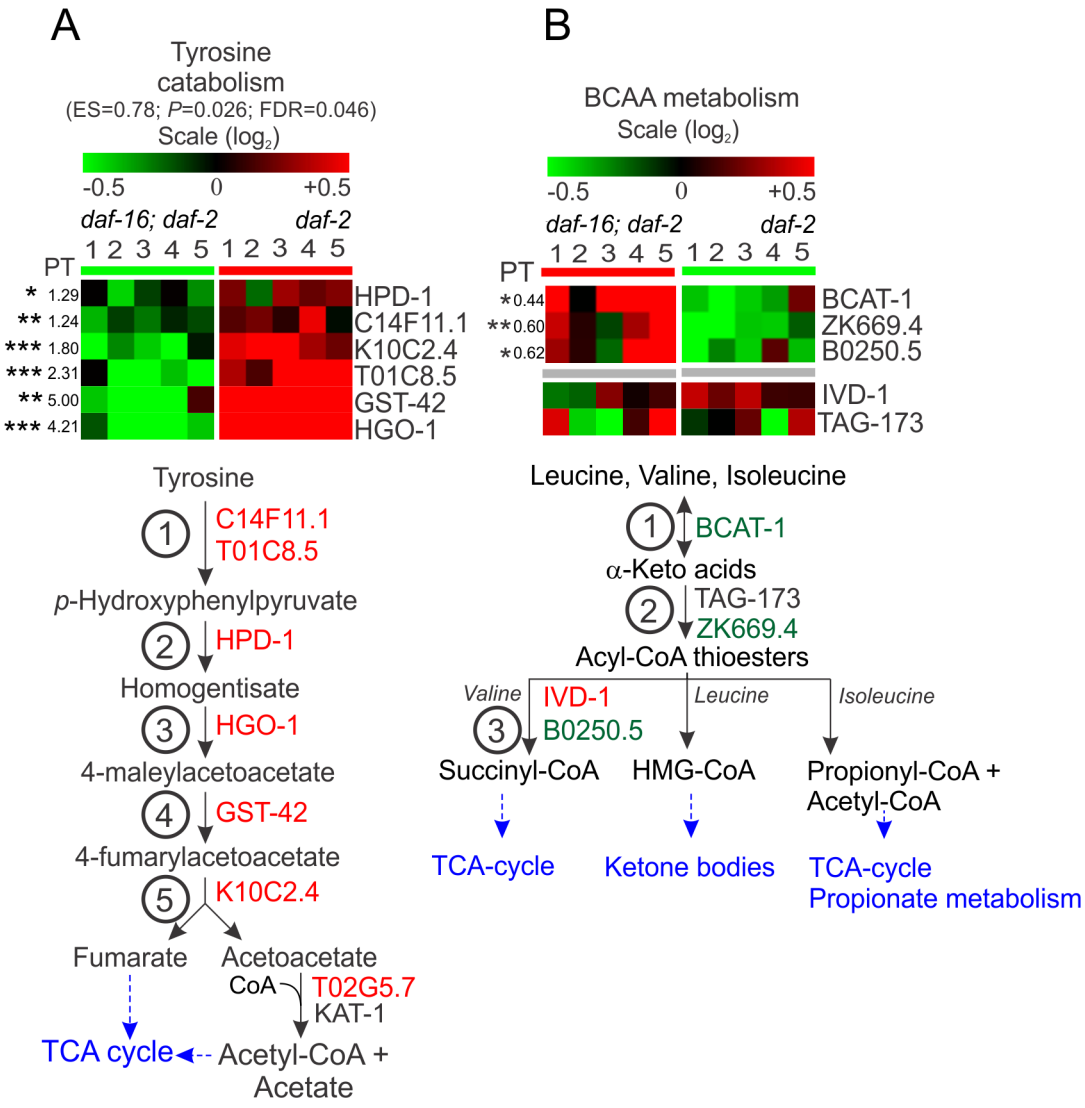

Figure 9. (A) Tyrosine catabolism. (Right) Heat map and (left) schematic overview of tyrosine catabolism enzymes. Numbers next to each heat map row denote fold change (linear) in abundance for statistically significant proteins. Proteins with significantly changed abundance levels are denoted *, $p < 0.05$; **, $p < 0.005$; and ***, $p < 0.0005$. (1) (Tyrosine/aspartate) transaminase, (2) *p*-hydroxyphenylpyruvate hydroxylase, (3) homogentisate oxidase, (4) maleylacetoacetate isomerase, and (5) fumarylacetoacetate hydrolase. (B) BCAA catabolism. (1) Branched-chain aminotransferase, (2) branched-chain α-keto acid decarboxylase complex, and (3) IVD-1, isovaryl-CoA dehydrogenase; B0250.5, 3-hydroxyisobutyrate dehydrogenase.

Interestingly, MAI-2, a member of the F1 ATPase inhibitor (IF1) family, showed a modest but significant upregulation in *daf-2* adults. IF1 inhibitor proteins prevent the deleterious hydrolytic consumption of ATP by complex V under anoxic conditions when the electrochemical gradient across the inner membrane collapses.[127] This finding is consistent with an earlier report of elevated transcriptional expression of IF1 inhibitors in *daf-2* mutants and dauers.[23] Increased expression of MAI-2 may, in part, explain the ability of *daf-2* to withstand prolonged hypoxic insult better.[8]

CONCLUSIONS

Decreased Gluconeogenic Flux in the Young Adult *daf-2* Mutant Is Suggestive of Increased Malate Dismutation

We found increased levels of most glycolytic enzymes (with the exception of pyruvate kinase) and gluconeogenic enzymes, including PEPCK. Together with an experimentally confirmed increased flux of carbon through the glyoxylate shunt and high levels of the storage sugars glycogen and trehalose, it was assumed gluconeogenic activity is high in the *daf-2* mutant. However, despite high PEPCK enzyme levels, a significant decrease of in vitro PEPCK activity was detected for the young adult *daf-2*, implying reduced gluconeogenesis. In contrast, pyruvate kinase activity was similar between *daf-2* and the *daf-16;daf-2* reference, suggesting glycolytic flux is not drastically altered in *daf-2*. In the event pyruvate kinase activity would be a limiting factor, the conversion of PEP into pyruvate is prevented, favoring glucose production via gluconeogenesis.[128−130] Alternatively, as was suggested by O'Riordan and Burnell, PEPCK potentially acts in reverse, driving CO_2 fixation via PEP and oxaloacetate with the subsequent formation of malate via malate dehydrogenase, as is seen in parasitic helminthes[97] (green arrows in Figure 1). Although increased levels of malate have been found in the *daf-2* mutant,[11] malate synthesis is most likely also increased via the upregulated glyoxylate shunt.

Helminths such as *Fasciola hepatica* and *Ascaris suum* are able to survive under anaerobic conditions in their host environment

dx.doi.org/10.1021/pr401081b | J. Proteome Res. 2014, 13, 1938−1956

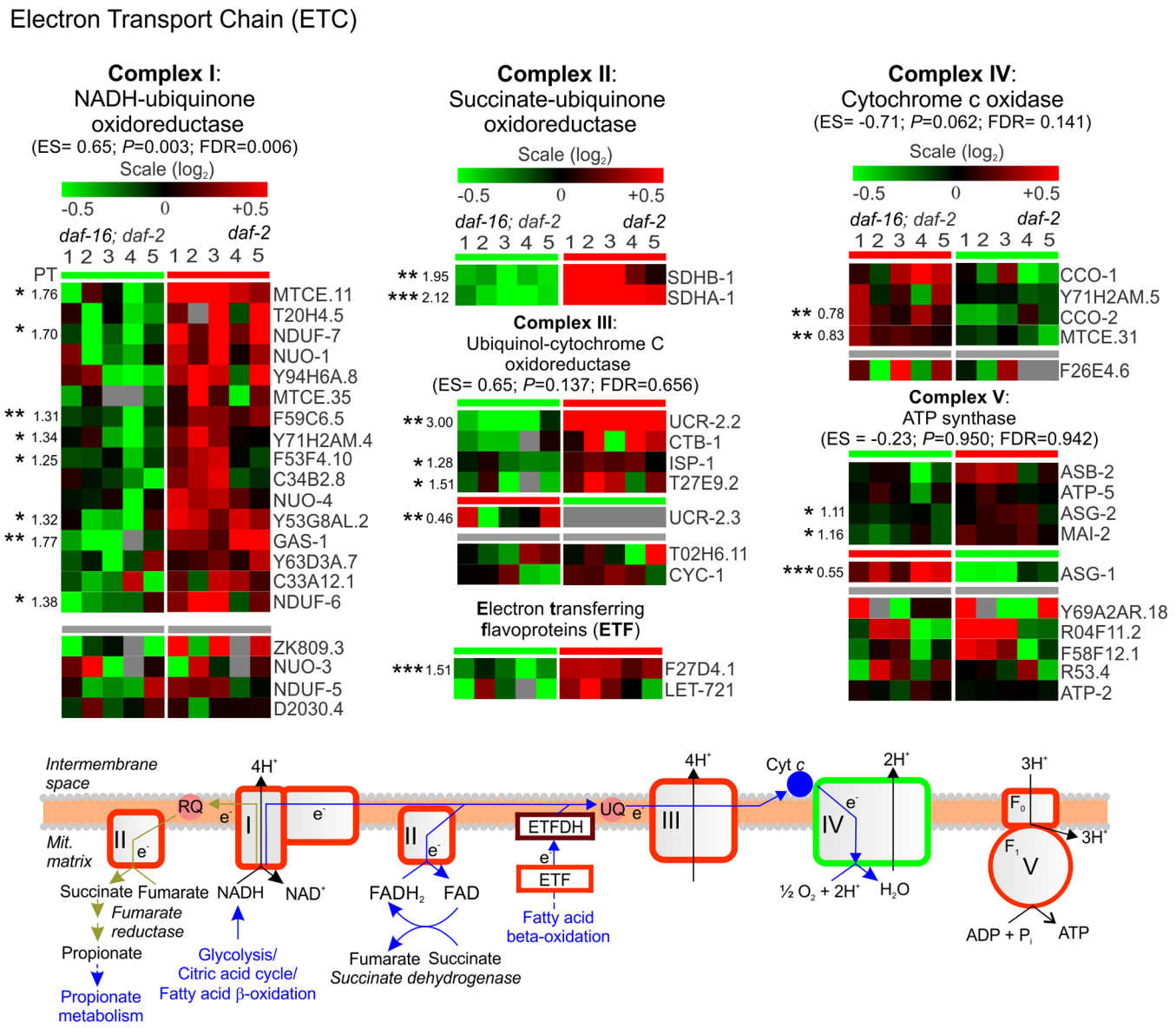

Figure 10. Mitochondrial respiratory chain. Schematic representation of the respiratory chain (Complexes I–IV) together with heat maps of detected subunits. Numbers next to each heat map row denote fold change (linear) in abundance for statistically significant proteins. Proteins with significantly changed abundance levels are denoted *, $p < 0.05$; **, $p < 0.005$; and ***, $p < 0.0005$. Green arrows indicate the possible alternative flux of electrons via rhodoquinone (RQ) (instead of ubiquinone, UQ) over complex II using fumarate as the final electron acceptor. ETF, electron transferring flavoprotein; ETFDH, electron transferring flavoprotein dehydrogenase.

by generating ATP via the malate dismutation pathway.[131,132] The malate dismutation pathway appears to be conserved in *C. elegans* and is thought to play an essential role in dauer energy metabolism and survival.[19,133] Furthermore, Rea and Johnson hypothesized that a shift from aerobic to mitochondrial anaerobic respiration underlies *daf-2* longevity and possibly most, if not all, other life-span extending mutations, including Mit mutants.[134] In this pathway, glycolytic phosphoenolpyruvate is converted into oxaloacetate by PEPCK, which is then further reduced by cytosolic malate dehydrogenase to produce malate. Once malate is transported into (partially) anaerobically functioning mitochondria, it is further catabolized to generate ATP from the proton gradient generated across the inner mitochondrial membrane by electron transport, but fumarate is utilized as the terminal electron acceptor instead of O_2, producing succinate instead of H_2O. We speculate the strong increased abundance of the putative mitochondrial tricarboxylate carrier K11H3.3 could be responsible for the increased import of cytosolic malate into the mitochondrial matrix in exchange for citrate (Figure 6b). As was noted earlier, strong activation of the glyoxylate shunt in *daf-2* mutants could also constitute a considerable source of intramitochondrial malate to drive anaerobic respiration. Although we were able to quantify several enzymes involved in malate dismutation, including malic enzyme (Y48B6A.12), ASC (C05C10.3), and STK subunits (C50F7.4, F47B10.1, and F23H11.3), none of them showed any significant alteration in protein expression (data not shown).

However, we detected a clear upregulation of all propionate catabolism enzymes in *daf-2*. Propionate is one of the principal waste products (along with acetate and succinate)[135] of malate dismutation and was previously found to be present in higher levels in the *daf-2* mutant.[13] Lastly, the conspicuous downregulation of complex IV components but increases in

dx.doi.org/10.1021/pr401081b | J. Proteome Res. 2014, 13, 1938–1956

complexes I–III could indicate that mitochondrial respiration in *daf-2* relies less on oxygen as the terminal electron acceptor to maintain the proton gradient. Taken together, these results support activation of the malate dismutation pathway in *daf-2*, a hypothesis that merits further study.

daf-2 Shares Altered One-Carbon Metabolism with the *pept-1* Mutant

Protein expression of enzymes in THF anabolism and the SAM biosynthetic pathway were increased and decreased in the *daf-2* mutant, respectively. Interestingly, previous proteomic and metabolomic analysis of the *pept-1* mutant revealed a very similar decrease in the abundance of one-carbon metabolism enzymes, including S-adenosylmethionine synthase (SAMS-1) and S-adenosylhomocysteine hydrolase (AHCY-1), and changes in methionine (decreased) and homocysteine (increased).[12] *pept-1* encodes an intestinal peptide transporter required for the absorption of amino acids in form of di- and tripeptides from the environment, and its mutation further extends *daf-2* lifespan by approximately 60%.[136] In contrast with our findings, however, the same group was unable to find these changes for the *daf-2* mutant. Nevertheless, reduced SAMS-1 protein levels in *daf-2* have been reported before,[67] and *daf-2* is characterized as a strong transcriptional repression of *pept-1*.[39] SAMS-1 was previously discovered to be a mediator of the DR response, possibly downstream of TOR signaling, and is required for a normal protein synthesis rate.[137,138] In addition, metformin-induced lifespan extension in *C. elegans* was recently shown to result from methionine restriction following disruption of folate metabolism in the *E. coli* food source.[139] Therefore, one attractive hypothesis is that alterations in the methionine cycle results in reduced protein synthesis in the *daf-2* mutant, the latter of which has been experimentally confirmed by us[47] and others.[140] By extension, we postulate decreased protein synthesis in the *pept-1* mutant and metformin-treated *C. elegans*, which could conceivably underlie their longevity phenotype.[141−143] Moreover, because RNAi knockdown of *pept-1* results in a significant decrease in the intracellular pool of free amino acids, a concomitant decrease in protein synthesis is to be expected.[12,136]

Altered Amino Acid Metabolism in the *daf-2* Mutant

Several metabolomic profiling studies have revealed changes in the metabolism of amino acids in the *daf-2* mutant.[11−13] In particular, changes in BCAA metabolism have been linked to *daf-2*, but it remains unclear how these changes contribute to *daf-2* longevity, if at all. In mammals, BCAAs (leucine in particular) are well-known to stimulate protein synthesis through activation of TOR (target of rapamycin) kinase.[144] However, because we recently showed that protein synthesis is repressed in the *daf-2* mutant, such action by BCAAs would thus have to be restricted to certain tissues, such as body-wall muscles, which we have shown previouslty are preserved from degradation in *daf-2*.[47] More recently, increased levels of aromatic amino acids (Phe and Tyr) and especially BCAA degradation products, such as Glu, Ala, and C3 and C5 acylcarnitines, were found to be strongly associated with insulin resistance and type 2 diabetes in humans.[145] It was suggested that accumulation of these incompletely oxidized intermediates causes mitochondrial stress, leading to impaired insulin action.[146] It is therefore conceivable that the rationale for the inhibition of BCAA catabolism in the *daf-2* mutant is a (futile) attempt to restore normal insulin/IGF-1 signaling levels. In parallel, tyrosine was identified in *C. elegans* as a potent antagonist of insulin signaling, promoting dauer formation and inducing longevity (A. Ferguson, P. Hu, D. Kim, and A. Fisher, personal communication), and enzymes of this pathway have been associated with *C. elegans* longevity before.[15,17,19,39,67,147] Similarly, the increased catabolism of tyrosine is conceivably part of a feedback mechanism for restoration of normal insulin/IGF-1 signaling. Finally, C3 and C5 acylcarnitines mainly arise from the incomplete catabolism of propionate (following BCAA degradation, Figure 8). Thus, increased expression of propionate catabolism enzymes should further prevent accumulation of these intermediates.

Does the *daf-2* Metabolic Pattern Also Support Its Long Lifespan?

Interestingly, attenuation of intermediary metabolism (glycolysis, the TCA cycle, and gluconeogenesis)[67,137,148−150] and the electron transport chain[15,151−153] has been reported to extend life-span of *daf-2* mutants significantly further. This is unexpected because expression of all these enzymes is increased in response to reduced IIS. It has been suggested that activation of metabolism is part of a compensatory mechanism triggered by reduced IIS that antagonizes full life-span potential of *daf-2* mutants.[67] We additionally propose that further attenuation of an already reduced metabolic rate could have an additive effect on *daf-2* lifespan, perhaps at the cost of reduced metabolic responsiveness to environmental triggers. Note, however, that activation of the glyoxylate shunt (isocitrate lyase/malate synthase, ICL-1) has been shown to be required for full life-span extension in the *daf-2* mutant[17] as well as in ubiquinone-defective *clk-1*,[103] suggesting that increased activity of this pathway is indispensable for IIS- or ETC-induced longevity.

In summary, our data suggests *daf-2* mutant cells are equipped with highly bioenergetic competent mitochondria and a proficient, partly rerouted metabolic network that makes economical use of internal energy stores to maintain energy homeostasis during its long life. A major challenge for the field will be to unravel the multiplicity of tissue-specific metabolic changes and how these tissues in turn interact to achieve the extensive physiological transformation induced by mutation in *daf-2*. Ultimately, such detailed understanding of the altered metabolism of *C. elegans* IIS mutants could also lead to important insights into various insulin-related disease pathologies in humans such as diabetes and obesity as well as aging.

■ ASSOCIATED CONTENT

Ⓢ Supporting Information

Details concerning individual proteomic samples, data sets used to build the AMT tag database, and SEQUEST data sets. Quantification of worm length, diameter, and volume. This material is available free of charge via the Internet at http://pubs.acs.org.

■ AUTHOR INFORMATION

Corresponding Author

*E-mail: Bart.Braeckman@UGent.be. Tel: +32.9.264.8744. Fax: +32.9.264.8793.

Author Contributions

§These authors contributed equally to this work.

Notes

The authors declare no competing financial interest.

■ ACKNOWLEDGMENTS

The strains GA154 *glp-4*(*bn2ts*)I;*daf-2*(*e1370*)III and GA153 *glp-4*(*bn2ts*)I *daf-16*(*mgDf50*)I;*daf-2*(*e1370*)III were kindly provided by David Gems. We are grateful to Renata Coopman for her assistance in culturing and sampling worm cohorts. We thank Ineke Dhondt and Myriam Claeys for providing transmission electron microcopy images, Caroline Vlaeminck for oil red O staining, and Patricia Back for assistance with image processing of stained nematodes. We thank all members of the Braeckman lab for helpful discussions and comments on the manuscript and David Gems for critical reading of the manuscript. This work was supported by a grant from the Fund for Scientific Research−Flanders (G.04371.0N to B.P.B.) and the NIH National Center for Research Resources (RR18522 to R.D.S.). G.D. was supported by a BOF project of Ghent University (01J04208). Proteomic analyses were performed in the Environmental Molecular Sciences Laboratory, a U.S. Department of Energy (DOE) national scientific user facility located at the Pacific Northwest National Laboratory (PNNL) in Richland, Washington. PNNL is a multiprogram national laboratory operated by Battelle for the DOE under contract DE-AC05-76RL01830.

■ ABBREVIATIONS

2D-DIGE, two-dimensional difference gel electrophoresis; 3PG, 3-phosphoglycerate; 4-HNE, 4-hydroxynonenal; ACL, ATP-citrate lyase; ACS, acetate:succinate CoA-transferase; AICAR, aminoimidazole carboxamide ribofuranoside; AT(D)P, adenosine-5′-tri(di)phosphate; CBS, cystathionine β-synthase; CoA, coenzyme A; DHAP, dihydroxyacetone phosphate; DIC, dicarboxylic acid carrier; DNA, deoxyribonucleic acid; ETC, electron transport chain; ETF, electron-transferring flavoprotein; ETFDH, electron-transferring flavoprotein dehydrogenase; $FADH_2$, flavin adenine dinucleotide; FOXO, forkhead box O; Fru-1,6-BP, fructose 1,6-bisphosphate; Fru-6P, fructose-6-phosphate; G3P, glyceraldehyde-3-phosphate; G6PDH, glucose-6-phosphate dehydrogenase; Glu-6P, glucose-6-phosphate; GSH/GSSG, reduced and oxidized glutathione, respectively; HMG, 3-hydroxy-3-methyl glutarate; IF1, F1 ATPase inhibitor; IGF-1, insulin-like growth factor-1; IIS, insulin/IGF-1 signaling; IRE, insulin responsive element; KEGG, Kyoto Encyclopedia of Genes and Genomes; LC−MS, liquid chromatography−mass spectrometry; mRNA, messenger ribonucleic acid; NADH, nicotinamide adenine dinucleotide NADPH, nicotinamide adenine dinucleotide phosphate; OOA, oxaloacetate; PEP, phosphoenol pyruvate; PEPCK, phosphoenol pyruvate carboxykinase; ROS, reactive oxygen species; RQ, rhodoquinone; SAGE, serial analysis of gene expression; SAH, S-adenosylhomocysteine; SAM, S-adenosyl methionine; SOD, superoxide dismutase; STK, succinate thiokinase; TAT, tyrosine aminotransferase; TEM, transmission electron microscopy; TCA, tricarboxylic acid; THF, tetrahydrofolate; TIC, tricarboxylate carrier; UQ, ubiquinone

■ REFERENCES

(1) Friedman, D. B.; Johnson, T. E. A mutation in the *age-1* gene in *Caenorhabditis elegans* lengthens life and reduces hermaphrodite fertility. *Genetics* **1988**, *118*, 75−86.

(2) Kenyon, C.; Chang, J.; Gensch, E.; Rudner, A.; Tabtiang, R. A *C. elegans* mutant that lives twice as long as wild-type. *Nature* **1993**, *366*, 461−464.

(3) Morris, J. Z.; Tissenbaum, H. A.; Ruvkun, G. A phosphatidylinositol-3-OH kinase family member regulating longevity and diapause in *Caenorhabditis elegans*. *Nature* **1996**, *382*, 536−539.

(4) Kimura, K. D.; Tissenbaum, H. A.; Liu, Y.; Ruvkun, G. *daf-2*, an insulin receptor-like gene that regulates longevity and diapause in *Caenorhabditis elegans*. *Science* **1997**, *277*, 942−946.

(5) Honda, Y.; Honda, S. The *daf-2* gene network for longevity regulates oxidative stress resistance and Mn-superoxide dismutase gene expression in *Caenorhabditis elegans*. *FASEB J.* **1999**, *13*, 1385−1393.

(6) Lithgow, G. J.; White, T. M.; Melov, S.; Johnson, T. E. Thermotolerance and extended life-span conferred by single-gene mutations and induced by thermal-stress. *Proc. Natl. Acad. Sci. U.S.A.* **1995**, *92*, 7540−7544.

(7) Garsin, D. A.; Villanueva, J. M.; Begun, J.; Kim, D. H.; Sifri, C. D.; Calderwood, S. B.; Ruvkun, G.; Ausubel, F. M. Long-lived *C. elegans daf-2* mutants are resistant to bacterial pathogens. *Science* **2003**, *300*, 1921−1921.

(8) Scott, B. A.; Avidan, M. S.; Crowder, C. M. Regulation of hypoxic death in *C. elegans* by the insulin/IGF receptor homolog DAF-2. *Science* **2002**, *296*, 2388−2391.

(9) Barsyte, D.; Lovejoy, D. A.; Lithgow, G. J. Longevity and heavy metal resistance in *daf-2* and *age-1* long-lived mutants of *Caenorhabditis elegans*. *FASEB J.* **2001**, *15*, 627−634.

(10) Houthoofd, K.; Braeckman, B. P.; Lenaerts, I.; Brys, K.; Matthijssens, F.; De Vreese, A.; Van Eygen, S.; Vanfleteren, J. R. DAF-2 pathway mutations and food restriction in aging *Caenorhabditis elegans* differentially affect metabolism. *Neurobiol. Aging* **2005**, *26*, 689−696.

(11) Castro, C.; Krumsiek, J.; Lehrbach, N. J.; Murfitt, S. A.; Miska, E. A.; Griffin, J. L. A study of *Caenorhabditis elegans* DAF-2 mutants by metabolomics and differential correlation networks. *Mol Biosyst* **2013**, *9*, 1632−1642.

(12) Martin, F. P.; Spanier, B.; Collino, S.; Montoliu, I.; Kolmeder, C.; Giesbertz, P.; Affolter, M.; Kussmann, M.; Daniel, H.; Kochhar, S.; Rezzi, S. Metabotyping of *Caenorhabditis elegans* and their culture media revealed unique metabolic phenotypes associated to amino acid deficiency and insulin-like signaling. *J. Proteome Res.* **2011**, *10*, 990−1003.

(13) Fuchs, S.; Bundy, J. G.; Davies, S. K.; Viney, J. M.; Swire, J. S.; Leroi, A. M. A metabolic signature of long life in *Caenorhabditis elegans*. *BMC Biol.* **2010**, *8*, 14-1−14-12.

(14) Halaschek-Wiener, J.; Khattra, J. S.; McKay, S.; Pouzyrev, A.; Stott, J. M.; Yang, G. S.; Holt, R. A.; Jones, S. J. M.; Marra, M. A.; Brooks-Wilson, A. R.; Riddle, D. L. Analysis of long-lived *C. elegans daf-2* mutants using serial analysis of gene expression. *Genome Res.* **2005**, *15*, 603−615.

(15) Lee, S. S.; Kennedy, S.; Tolonen, A. C.; Ruvkun, G. DAF-16 target genes that control *C. elegans* life-span and metabolism. *Science* **2003**, *300*, 644−647.

(16) McElwee, J.; Bubb, K.; Thomas, J. H. Transcriptional outputs of the *Caenorhabditis elegans* forkhead protein DAF-16. *Aging Cell* **2003**, *2*, 111−121.

(17) Murphy, C. T.; McCarroll, S. A.; Bargmann, C. I.; Fraser, A.; Kamath, R. S.; Ahringer, J.; Li, H.; Kenyon, C. Genes that act downstream of DAF-16 to influence the lifespan of *Caenorhabditis elegans*. *Nature* **2003**, *424*, 277−283.

(18) Ruzanov, P.; Riddle, D. L.; Marra, M. A.; McKay, S. J.; Jones, S. M. Genes that may modulate longevity in *C. elegans* in both dauer larvae and long-lived *daf-2* adults. *Exp. Gerontol.* **2007**, *42*, 825−839.

(19) Holt, S. J.; Riddle, D. L. SAGE surveys *C. elegans* carbohydrate metabolism: Evidence for an anaerobic shift in the long-lived dauer larva. *Mech. Ageing Dev.* **2003**, *124*, 779−800.

(20) Holt, S. J. Staying alive in adversity: Transcriptome dynamics in the stress-resistant dauer larva. *Funct. Integr. Genomics* **2006**, *6*, 285−299.

(21) Jones, S. J.; Riddle, D. L.; Pouzyrev, A. T.; Velculescu, V. E.; Hillier, L.; Eddy, S. R.; Stricklin, S. L.; Baillie, D. L.; Waterston, R.; Marra, M. A. Changes in gene expression associated with

developmental arrest and longevity in *Caenorhabditis elegans*. *Genome Res.* **2001**, *11*, 1346−1352.
(22) Wang, J.; Kim, S. K. Global analysis of dauer gene expression in *Caenorhabditis elegans*. *Development* **2003**, *130*, 1621−1634.
(23) McElwee, J. J.; Schuster, E.; Blanc, E.; Thornton, J.; Gems, D. Diapause-associated metabolic traits reiterated in long-lived *daf-2* mutants in the nematode *Caenorhabditis elegans*. *Mech. Ageing Dev.* **2006**, *127*, 458−472.
(24) Shaw, W. M.; Luo, S.; Landis, J.; Ashraf, J.; Murphy, C. T. The *C. elegans* TGF-beta dauer pathway regulates longevity via insulin signaling. *Curr. Biol.* **2007**, *17*, 1635−1645.
(25) Pagotto, U. Where does insulin resistance start? The brain. *Diabetes Care* **2009**, *32*, S174−S177.
(26) Carvalheira, J. B.; Ribeiro, E. B.; Araujo, E. P.; Guimaraes, R. B.; Telles, M. M.; Torsoni, M.; Gontijo, J. A.; Velloso, L. A.; Saad, M. J. Selective impairment of insulin signalling in the hypothalamus of obese Zucker rats. *Diabetologia* **2003**, *46*, 1629−1640.
(27) Obici, S.; Feng, Z.; Karkanias, G.; Baskin, D. G.; Rossetti, L. Decreasing hypothalamic insulin receptors causes hyperphagia and insulin resistance in rats. *Nat. Neurosci.* **2002**, *5*, 566−572.
(28) Sipols, A. J.; Baskin, D. G.; Schwartz, M. W. Effect of intracerebroventricular insulin infusion on diabetic hyperphagia and hypothalamic neuropeptide gene expression. *Diabetes* **1995**, *44*, 147−151.
(29) Bruning, J. C.; Gautam, D.; Burks, D. J.; Gillette, J.; Schubert, M.; Orban, P. C.; Klein, R.; Krone, W.; Muller-Wieland, D.; Kahn, C. R. Role of brain insulin receptor in control of body weight and reproduction. *Science* **2000**, *289*, 2122−2125.
(30) Wolkow, C. A.; Kimura, K. D.; Lee, M. S.; Ruvkun, G. Regulation of *C. elegans* life-span by insulinlike signaling in the nervous system. *Science* **2000**, *290*, 147−150.
(31) Pawlikowska, L.; Hu, D.; Huntsman, S.; Sung, A.; Chu, C.; Chen, J.; Joyner, A. H.; Schork, N. J.; Hsueh, W. C.; Reiner, A. P.; Psaty, B. M.; Atzmon, G.; Barzilai, N.; Cummings, S. R.; Browner, W. S.; Kwok, P. Y.; Ziv, E. Association of common genetic variation in the insulin/IGF1 signaling pathway with human longevity. *Aging Cell* **2009**, *8*, 460−472.
(32) Kojima, T.; Kamei, H.; Aizu, T.; Arai, Y.; Takayama, M.; Nakazawa, S.; Ebihara, Y.; Inagaki, H.; Masui, Y.; Gondo, Y.; Sakaki, Y.; Hirose, N. Association analysis between longevity in the Japanese population and polymorphic variants of genes involved in insulin and insulin-like growth factor 1 signaling pathways. *Exp. Gerontol.* **2004**, *39*, 1595−1598.
(33) Kappeler, L.; De Magalhaes Filho, C.; Dupont, J.; Leneuve, P.; Cervera, P.; Perin, L.; Loudes, C.; Blaise, A.; Klein, R.; Epelbaum, J.; Le Bouc, Y.; Holzenberger, M. Brain IGF-1 receptors control mammalian growth and lifespan through a neuroendocrine mechanism. *PLoS Biol.* **2008**, *6*, e254-1−e254-10.
(34) Selman, C.; Lingard, S.; Choudhury, A. I.; Batterham, R. L.; Claret, M.; Clements, M.; Ramadani, F.; Okkenhaug, K.; Schuster, E.; Blanc, E.; Piper, M. D.; Al-Qassab, H.; Speakman, J. R.; Carmignac, D.; Robinson, I. C.; Thornton, J. M.; Gems, D.; Partridge, L.; Withers, D. J. Evidence for lifespan extension and delayed age-related biomarkers in insulin receptor substrate 1 null mice. *FASEB J.* **2008**, *22*, 807−818.
(35) Suh, Y.; Atzmon, G.; Cho, M. O.; Hwang, D.; Liu, B.; Leahy, D. J.; Barzilai, N.; Cohen, P. Functionally significant insulin-like growth factor I receptor mutations in centenarians. *Proc. Natl. Acad. Sci. U.S.A.* **2008**, *105*, 3438−3442.
(36) Kaletta, T.; Hengartner, M. O. Finding function in novel targets: *C. elegans* as a model organism. *Nat. Rev. Drug Discovery* **2006**, *5*, 387−398.
(37) Markaki, M.; Tavernarakis, N. Modeling human diseases in *Caenorhabditis elegans*. *Biotechnol. J.* **2010**, *5*, 1261−76.
(38) Ruzanov, P.; Riddle, D. L. Deep SAGE analysis of the *Caenorhabditis elegans* transcriptome. *Nucleic Acids Res.* **2010**, *38*, 3252−3262.
(39) McElwee, J. J.; Schuster, E.; Blanc, E.; Thomas, J. H.; Gems, D. Shared transcriptional signature in *Caenorhabditis elegans* dauer larvae and long-lived *daf-2* mutants implicates detoxification system in longevity assurance. *J. Biol. Chem.* **2004**, *279*, 44533−44543.
(40) Murphy, C. T. The search for DAF-16/FOXO transcriptional targets: Approaches and discoveries. *Exp. Gerontol.* **2006**, *41*, 910−921.
(41) McKay, S. J.; Johnsen, R.; Khattra, J.; Asano, J.; Baillie, D. L.; Chan, S.; Dube, N.; Fang, L.; Goszczynski, B.; Ha, E.; Halfnight, E.; Hollebakken, R.; Huang, P.; Hung, K.; Jensen, V.; Jones, S. J.; Kai, H.; Li, D.; Mah, A.; Marra, M.; McGhee, J.; Newbury, R.; Pouzyrev, A.; Riddle, D. L.; Sonnhammer, E.; Tian, H.; Tu, D.; Tyson, J. R.; Vatcher, G.; Warner, A.; Wong, K.; Zhao, Z.; Moerman, D. G. Gene expression profiling of cells, tissues, and developmental stages of the nematode *C. elegans*. *Cold Spring Harbor Symp. Quant. Biol.* **2003**, *68*, 159−169.
(42) Tian, Q.; Stepaniants, S. B.; Mao, M.; Weng, L.; Feetham, M. C.; Doyle, M. J.; Yi, E. C.; Dai, H. Y.; Thorsson, V.; Eng, J.; Goodlett, D.; Berger, J. P.; Gunter, B.; Linseley, P. S.; Stoughton, R. B.; Aebersold, R.; Collins, S. J.; Hanlon, W. A.; Hood, L. E. Integrated genomic and proteomic analyses of gene expression in mammalian cells. *Mol. Cell. Proteomics* **2004**, *3*, 960−969.
(43) Maier, T.; Guell, M.; Serrano, L. Correlation of mRNA and protein in complex biological samples. *FEBS Lett.* **2009**, *583*, 3966−3973.
(44) Beanan, M. J.; Strome, S. Characterization of a germ-line proliferation mutation in *C. elegans*. *Development* **1992**, *116*, 755−766.
(45) TeKippe, M.; Aballay, A. *C. elegans* germline-deficient mutants respond to pathogen infection using shared and distinct mechanisms. *PLoS One* **2010**, *5*, e11777-1−e11777-9.
(46) Krijgsveld, J.; Ketting, R. F.; Mahmoudi, T.; Johansen, J.; Artal-Sanz, M.; Verrijzer, C. P.; Plasterk, R. H.; Heck, A. J. Metabolic labeling of *C. elegans* and *D. melanogaster* for quantitative proteomics. *Nat. Biotechnol.* **2003**, *21*, 927−931.
(47) Depuydt, G.; Xie, F.; Petyuk, V. A.; Shanmugam, N.; Smolders, A.; Dhondt, I.; Brewer, H. M.; Camp, D. G.; Smith, R. D.; Braeckman, B. P. Reduced insulin/IGF-1 signaling and dietary restriction inhibit translation but preserve muscle mass in *Caenorhabditis elegans*. *Mol. Cell. Proteomics* **2013**, *12*, 3624−3639.
(48) Desiere, F.; Deutsch, E. W.; King, N. L.; Nesvizhskii, A. I.; Mallick, P.; Eng, J.; Chen, S.; Eddes, J.; Loevenich, S. N.; Aebersold, R. The PeptideAtlas project. *Nucleic Acids Res.* **2006**, *34*, D655−D658.
(49) Saeed, A. I.; Bhagabati, N. K.; Braisted, J. C.; Liang, W.; Sharov, V.; Howe, E. A.; Li, J.; Thiagarajan, M.; White, J. A.; Quackenbush, J. TM4 microarray software suite. *Methods Enzymol.* **2006**, *411*, 134−193.
(50) Saeed, A. I.; Sharov, V.; White, J.; Li, J.; Liang, W.; Bhagabati, N.; Braisted, J.; Klapa, M.; Currier, T.; Thiagarajan, M.; Sturn, A.; Snuffin, M.; Rezantsev, A.; Popov, D.; Ryltsov, A.; Kostukovich, E.; Borisovsky, I.; Liu, Z.; Vinsavich, A.; Trush, V.; Quackenbush, J. TM4: A free, open-source system for microarray data management and analysis. *Biotechniques* **2003**, *34*, 374−378.
(51) Pavlidis, P.; Noble, W. S. Analysis of strain and regional variation in gene expression in mouse brain. *Genome Biol.* **2001**, *2*, RESEARCH0042-1−RESEARCH0042-15.
(52) Kanehisa, M.; Goto, S.; Sato, Y.; Furumichi, M.; Tanabe, M. KEGG for integration and interpretation of large-scale molecular data sets. *Nucleic Acids Res.* **2011**, *40*, D109−D114.
(53) Magrane, M.; Consortium, U. UniProt Knowledgebase: A hub of integrated protein data. *Database* **2011**, *2011*, bar009-1−bar009-13.
(54) Subramanian, A.; Tamayo, P.; Mootha, V. K.; Mukherjee, S.; Ebert, B. L.; Gillette, M. A.; Paulovich, A.; Pomeroy, S. L.; Golub, T. R.; Lander, E. S.; Mesirov, J. P. Gene set enrichment analysis: A knowledge-based approach for interpreting genome-wide expression profiles. *Proc. Natl. Acad. Sci. U.S.A.* **2005**, *102*, 15545−15550.
(55) Fonderie, P.; Willems, M.; Bert, W.; Houthoofd, W.; Steel, H.; Claeys, M.; Borgonie, G. Intestine ultrastructure of the facultative parasite *Halicephalobus gingivalis* (Nematoda: Panagrolaimidae). *Nematology* **2009**, *11*, 859−868.
(56) O'Rourke, E. J.; Soukas, A. A.; Carr, C. E.; Ruvkun, G. *C. elegans* major fats are stored in vesicles distinct from lysosome-related organelles. *Cell Metab.* **2009**, *10*, 430−435.

(57) Fiji Image Processing Package Home Page. http://fiji.sc/wiki/index.php/Fiji.
(58) Castelein, N.; Hoogewijs, D.; De Vreese, A.; Braeckman, B. P.; Vanfleteren, J. R. Dietary restriction by growth in axenic medium induces discrete changes in the transcriptional output of genes involved in energy metabolism in *Caenorhabditis elegans*. *Biotechnol. J.* **2008**, *3*, 803−812.
(59) *Methods of Enzymatic Analysis*; Bergmeyer, H. U., Ed.; Academic Press: New York, 1974; pp 500−501.
(60) Racker, E. Spectrophotometric measurements of the enzymatic formation of fumaric and cis-aconitic acids. *Biochim. Biophys. Acta* **1950**, *4*, 211−214.
(61) Lynen, F.; Wieland, O. Beta-ketoreductase. *Methods Enzymol.* **1955**, *1*, 566−573.
(62) Huang da, W.; Sherman, B. T.; Lempicki, R. A. Systematic and integrative analysis of large gene lists using DAVID bioinformatics resources. *Nat. Protoc.* **2009**, *4*, 44−57.
(63) Huang da, W.; Sherman, B. T.; Lempicki, R. A. Bioinformatics enrichment tools: Paths toward the comprehensive functional analysis of large gene lists. *Nucleic Acids Res.* **2009**, *37*, 1−13.
(64) Murray, R. K.; Granner, D. K.; Mayes, P. A.; Rodwell, V. W. *Harper's Illustrated Biochemistry*, 25th ed.; McGraw-Hill: New York, 2000; p 927.
(65) Chakravarty, K.; Cassuto, H.; Reshef, L.; Hanson, R. W. Factors that control the tissue-specific transcription of the gene for phosphoenolpyruvate carboxykinase-C. *Crit. Rev. Biochem. Mol. Biol.* **2005**, *40*, 129−154.
(66) Tazearslan, C.; Ayyadevara, S.; Bharill, P.; Shmookler Reis, R. J. Positive feedback between transcriptional and kinase suppression in nematodes with extraordinary longevity and stress resistance. *PLoS Genet.* **2009**, *5*, e1000452-1−e1000452-15.
(67) Dong, M. Q.; Venable, J. D.; Au, N.; Xu, T.; Park, S. K.; Cociorva, D.; Johnson, J. R.; Dillin, A.; Yates, J. R., 3rd Quantitative mass spectrometry identifies insulin signaling targets in *C. elegans*. *Science* **2007**, *317*, 660−663.
(68) Brys, K.; Castelein, N.; Matthijssens, F.; Vanfleteren, J. R.; Braeckman, B. P. Disruption of insulin signalling preserves bioenergetic competence of mitochondria in ageing *Caenorhabditis elegans*. *BMC Biol.* **2010**, *8*, 91-1−91-15.
(69) Frazier, H. N., 3rd; Roth, M. B. Adaptive sugar provisioning controls survival of *C. elegans* embryos in adverse environments. *Curr. Biol.* **2009**, *19*, 859−863.
(70) Popham, J. D.; Webster, J. M. Aspects of the fine-structure of the dauer larva of the nematode *Caenorhabditis elegans*. *Can. J. Zool.* **1979**, *57*, 794−800.
(71) Foll, R. L.; Pleyers, A.; Lewandovski, G. J.; Wermter, C.; Hegemann, V.; Paul, R. J. Anaerobiosis in the nematode *Caenorhabditis elegans*. *Comp. Biochem. Physiol., Part B: Biochem. Mol. Biol.* **1999**, *124*, 269−280.
(72) Burnell, A. M.; Houthoofd, K.; O'Hanlon, K.; Vanfleteren, J. R. Alternate metabolism during the dauer stage of the nematode *Caenorhabditis elegans*. *Exp. Gerontol.* **2005**, *40*, 850−856.
(73) Roy, P. J.; Stuart, J. M.; Lund, J.; Kim, S. K. Chromosomal clustering of muscle-expressed genes in *Caenorhabditis elegans*. *Nature* **2002**, *418*, 975−979.
(74) Honda, Y.; Tanaka, M.; Honda, S. Trehalose extends longevity in the nematode *Caenorhabditis elegans*. *Aging Cell* **2010**, *9*, 558−569.
(75) Lamitina, S. T.; Strange, K. Transcriptional targets of DAF-16 insulin signaling pathway protect *C. elegans* from extreme hypertonic stress. *Am. J. Physiol.: Cell Physiol.* **2005**, *288*, C467−C474.
(76) Pellerone, F. I.; Archer, S. K.; Behm, C. A.; Grant, W. N.; Lacey, M. J.; Somerville, A. C. Trehalose metabolism genes in *Caenorhabditis elegans* and filarial nematodes. *Int. J. Parasitol.* **2003**, *33*, 1195−1206.
(77) Hanover, J. A.; Forsythe, M. E.; Hennessey, P. T.; Brodigan, T. M.; Love, D. C.; Ashwell, G.; Krause, M. A *Caenorhabditis elegans* model of insulin resistance: Altered macronutrient storage and dauer formation in an OGT-1 knockout. *Proc. Natl. Acad. Sci. U.S.A.* **2005**, *102*, 11266−11271.
(78) Behm, C. A. The role of trehalose in the physiology of nematodes. *Int. J. Parasitol.* **1997**, *27*, 215−229.
(79) Hottiger, T.; De Virgilio, C.; Hall, M. N.; Boller, T.; Wiemken, A. The role of trehalose synthesis for the acquisition of thermotolerance in yeast. II. Physiological concentrations of trehalose increase the thermal stability of proteins in vitro. *Eur. J. Biochem.* **1994**, *219*, 187−193.
(80) Jain, N. K.; Roy, I. Effect of trehalose on protein structure. *Protein Sci.* **2009**, *18*, 24−36.
(81) Erkut, C.; Penkov, S.; Khesbak, H.; Vorkel, D.; Verbavatz, J. M.; Fahmy, K.; Kurzchalia, T. V. Trehalose renders the dauer larva of *Caenorhabditis elegans* resistant to extreme desiccation. *Curr. Biol.* **2011**, *21*, 1331−1336.
(82) Ralser, M.; Wamelink, M. M.; Kowald, A.; Gerisch, B.; Heeren, G.; Struys, E. A.; Klipp, E.; Jakobs, C.; Breitenbach, M.; Lehrach, H.; Krobitsch, S. Dynamic rerouting of the carbohydrate flux is key to counteracting oxidative stress. *J. Biol.* **2007**, *6*, 10-1−10-18.
(83) Legan, S. K.; Rebrin, I.; Mockett, R. J.; Radyuk, S. N.; Klichko, V. I.; Sohal, R. S.; Orr, W. C. Overexpression of glucose-6-phosphate dehydrogenase extends the life span of *Drosophila melanogaster*. *J. Biol. Chem.* **2008**, *283*, 32492−32499.
(84) Greenberg, J. T.; Monach, P.; Chou, J. H.; Josephy, P. D.; Demple, B. Positive control of a global antioxidant defense regulon activated by superoxide-generating agents in *Escherichia coli*. *Proc. Natl. Acad. Sci. U.S.A.* **1990**, *87*, 6181−6185.
(85) Schnell, N.; Krems, B.; Entian, K. D. The PAR1 (YAP1/SNQ3) gene of *Saccharomyces cerevisiae*, a c-jun homologue, is involved in oxygen metabolism. *Curr. Genet.* **1992**, *21*, 269−273.
(86) Kennedy, K. A.; Crouch, L. S.; Warshaw, J. B. Effect of hyperoxia on antioxidants in neonatal rat type II cells in vitro and in vivo. *Pediatr. Res.* **1989**, *26*, 400−403.
(87) Glasner, J. D.; Kocher, T. D.; Collins, J. J. *Caenorhabditis elegans* contains genes encoding 2 new members of the Zn-containing alcohol-dehydrogenase family. *J. Mol. Evol.* **1995**, *41*, 46−53.
(88) Alaimo, J. T.; Davis, S. J.; Song, S. S.; Burnette, C. R.; Grotewiel, M.; Shelton, K. L.; Pierce-Shimomura, J. T.; Davies, A. G.; Bettinger, J. C. Ethanol metabolism and osmolarity modify behavioral responses to ethanol in *C. elegans*. *Alcohol.: Clin. Exp. Res.* **2012**, *36*, 1840−1850.
(89) Madi, A.; Mikkat, S.; Koy, C.; Ringel, B.; Thiesen, H. J.; Glocker, M. O. Mass spectrometric proteome analysis suggests anaerobic shift in metabolism of dauer larvae of *Caenorhabditis elegans*. *Biochim. Biophys. Acta* **2008**, *1784*, 1763−1770.
(90) Bogaerts, A.; Beets, I.; Temmerman, L.; Schoofs, L.; Verleyen, P. Proteome changes of *Caenorhabditis elegans* upon a *Staphylococcus aureus* infection. *Biol. Direct* **2010**, 5-1−5-17.
(91) Bogaerts, A.; Temmerman, L.; Boerjan, B.; Husson, S. J.; Schoofs, L.; Verleyen, P. A differential proteomics study of *Caenorhabditis elegans* infected with *Aeromonas hydrophila*. *Dev. Comp. Immunol.* **2010**, *34*, 690−698.
(92) Boleda, M. D.; Saubi, N.; Farres, J.; Pares, X. Physiological substrates for rat alcohol dehydrogenase classes: Aldehydes of lipid peroxidation, omega-hydroxyfatty acids, and retinoids. *Arch. Biochem. Biophys.* **1993**, *307*, 85−90.
(93) Sellin, S.; Holmquist, B.; Mannervik, B.; Vallee, B. L. Oxidation and reduction of 4-hydroxyalkenals catalyzed by isozymes of human alcohol dehydrogenase. *Biochemistry* **1991**, *30*, 2514−2518.
(94) Singh, S. P.; Niemczyk, M.; Zimniak, L.; Zimniak, P. Fat accumulation in *Caenorhabditis elegans* triggered by the electrophilic lipid peroxidation product 4-hydroxynonenal (4-HNE). *Aging* **2009**, *1*, 68−80.
(95) Petersen, D. R.; Doorn, J. A. Reactions of 4-hydroxynonenal with proteins and cellular targets. *Free Radical Biol. Med.* **2004**, *37*, 937−945.
(96) Mitchell, D. Y.; Petersen, D. R. The oxidation of alpha-beta unsaturated aldehydic products of lipid peroxidation by rat liver aldehyde dehydrogenases. *Toxicol. Appl. Pharmacol.* **1987**, *87*, 403−410.
(97) O'Riordan, V. B.; Burnell, A. M. Intermediary metabolism in the dauer larva of the nematode *Caenorhabditis elegans* 0.1. Glycolysis,

gluconeogenesis, oxidative-phosphorylation and the tricarboxylic-acid cycle. *Comp. Biochem. Physiol., Part B: Biochem. Mol. Biol.* **1989**, *92*, 233−238.
(98) Vanfleteren, J. R.; Devreese, A. The gerontogenes *age-1* and *daf-2* determine metabolic-rate potential in aging *Caenorhabditis elegans*. *FASEB J.* **1995**, *9*, 1355−1361.
(99) Kim, Y. I.; Cho, J. H.; Yoo, O. J.; Ahnn, J. Transcriptional regulation and life-span modulation of cytosolic aconitase and ferritin genes in *C. elegans*. *J. Mol. Biol.* **2004**, *342*, 421−433.
(100) Vanni, P.; Giachetti, E.; Pinzauti, G.; Mcfadden, B. A. Comparative structure, function and regulation of isocitrate lyase, an important assimilatory enzyme. *Comp. Biochem. Physiol., Part B: Biochem. Mol. Biol.* **1990**, *95*, 431−458.
(101) Kahn, F. R.; McFadden, B. A. Embryogenesis and the glyoxylate cycle. *FEBS Lett.* **1980**, *115*, 312−314.
(102) Cristina, D.; Cary, M.; Lunceford, A.; Clarke, C.; Kenyon, C. A regulated response to impaired respiration slows behavioral rates and increases lifespan in *Caenorhabditis elegans*. *PLoS Genet.* **2009**, *5*, e1000450-1−e1000450-15.
(103) Gallo, M.; Park, D.; Riddle, D. L. Increased longevity of some *C. elegans* mitochondrial mutants explained by activation of an alternative energy-producing pathway. *Mech. Ageing Dev.* **2011**, *132*, 515−518.
(104) Liu, F.; Thatcher, J. D.; Barral, J. M.; Epstein, H. F. Bifunctional glyoxylate cycle protein of *Caenorhabditis elegans*: A developmentally regulated protein of intestine and muscle. *Dev. Biol.* **1995**, *169*, 399−414.
(105) Arinze, I. J. Facilitating understanding of the purine nucleotide cycle and the one-carbon pool: Part I: The purine nucleotide cycle. *Biochem. Mol. Biol. Educ.* **2005**, *33*, 165−168.
(106) Herbig, K.; Chiang, E. P.; Lee, L. R.; Hills, J.; Shane, B.; Stover, P. J. Cytoplasmic serine hydroxymethyltransferase mediates competition between folate-dependent deoxyribonucleotide and S-adenosylmethionine biosyntheses. *J. Biol. Chem.* **2002**, *277*, 38381−38389.
(107) Cook, R. J. Defining the steps of the folate one-carbon shuffle and homocysteine metabolism. *Am. J. Clin. Nutr.* **2000**, *72*, 1419−1420.
(108) Finkelstein, J. D. Metabolic regulatory properties of S-adenosylmethionine and S-adenosylhomocysteine. *Clin. Chem. Lab. Med.* **2007**, *45*, 1694−1699.
(109) Stipanuk, M. H.; Ueki, I. Dealing with methionine/homocysteine sulfur: Cysteine metabolism to taurine and inorganic sulfur. *J. Inherited Metab. Dis.* **2011**, *34*, 17−32.
(110) Mizuarai, S.; Miki, S.; Araki, H.; Takahashi, K.; Kotani, H. Identification of dicarboxylate carrier Slc25a10 as malate transporter in de novo fatty acid synthesis. *J. Biol. Chem.* **2005**, *280*, 32434−32441.
(111) Sun, T.; Hayakawa, K.; Bateman, K. S.; Fraser, M. E. Identification of the citrate-binding site of human ATP-citrate lyase using X-ray crystallography. *J. Biol. Chem.* **2010**, *285*, 27418−27428.
(112) Infantino, V.; Iacobazzi, V.; De Santis, F.; Mastrapasqua, M.; Palmieri, F. Transcription of the mitochondrial citrate carrier gene: Role of SREBP-1, upregulation by insulin and downregulation by PUFA. *Biochem. Biophys. Res. Commun.* **2007**, *356*, 249−254.
(113) Guay, C.; Madiraju, S. R.; Aumais, A.; Joly, E.; Prentki, M. A role for ATP-citrate lyase, malic enzyme, and pyruvate/citrate cycling in glucose-induced insulin secretion. *J. Biol. Chem.* **2007**, *282*, 35657−35665.
(114) Narbonne, P.; Roy, R. *Caenorhabditis elegans* dauers need LKB1/AMPK to ration lipid reserves and ensure long-term survival. *Nature* **2009**, *457*, 210−214.
(115) O'Riordan, V. B.; Burnell, A. M. Intermediary metabolism in the dauer larva of the nematode *Caenorhabditis elegans* 0.2. The glyoxylate cycle and fatty-acid oxidation. *Comp. Biochem. Physiol., Part B: Biochem. Mol. Biol.* **1990**, *95*, 125−130.
(116) Narbonne, P.; Roy, R. Inhibition of germline proliferation during *C. elegans* dauer development requires PTEN, LKB1 and AMPK signalling. *Development* **2006**, *133*, 611−619.
(117) Chandler, R. J.; Aswani, V.; Tsai, M. S.; Falk, M.; Wehrli, N.; Stabler, S.; Allen, R.; Sedensky, M.; Kazazian, H. H.; Venditti, C. P. Propionyl-CoA and adenosylcobalamin metabolism in *Caenorhabditis elegans*: Evidence for a role of methylmalonyl-CoA epimerase in intermediary metabolism. *Mol. Genet. Metab.* **2006**, *89*, 64−73.
(118) Kuhnl, J.; Bobik, T.; Procter, J. B.; Burmeister, C.; Hoppner, J.; Wilde, I.; Luersen, K.; Torda, A. E.; Walter, R. D.; Liebau, E. Functional analysis of the methylmalonyl-CoA epimerase from *Caenorhabditis elegans*. *FEBS J.* **2005**, *272*, 1465−1477.
(119) Fisher, A. L.; Page, K. E.; Lithgow, G. J.; Nash, L. The *Caenorhabditis elegans* K10C2.4 gene encodes a member of the fumarylacetoacetate hydrolase family: A *Caenorhabditis elegans* model of type I tyrosinemia. *J. Biol. Chem.* **2008**, *283*, 9127−9135.
(120) Durham, S. K.; Suwanichkul, A.; Scheimann, A. O.; Yee, D.; Jackson, J. G.; Barr, F. G.; Powell, D. R. FKHR binds the insulin response element in the insulin-like growth factor binding protein-1 promoter. *Endocrinology* **1999**, *140*, 3140−3146.
(121) Van Voorhies, W. A.; Ward, S. Genetic and environmental conditions that increase longevity in *Caenorhabditis elegans* decrease metabolic rate. *Proc. Natl. Acad. Sci. U.S.A.* **1999**, *96*, 11399−11403.
(122) Braeckman, B. P.; Houthoofd, K.; Vanfleteren, J. R. Assessing metabolic activity in aging *Caenorhabditis elegans*: Concepts and controversies. *Aging Cell* **2002**, *1*, 82−88 discussion 102−103.
(123) Hsu, A. L.; Feng, Z.; Hsieh, M. Y.; Xu, X. Z. Identification by machine vision of the rate of motor activity decline as a lifespan predictor in *C. elegans*. *Neurobiol. Aging* **2009**, *30*, 1498−1503.
(124) Gaglia, M. M.; Kenyon, C. Stimulation of movement in a quiescent, hibernation-like form of *Caenorhabditis elegans* by dopamine signaling. *J. Neurosci.* **2009**, *29*, 7302−7314.
(125) Cassada, R. C.; Russell, R. L. The dauerlarva, a post-embryonic developmental variant of the nematode *Caenorhabditis elegans*. *Dev. Biol.* **1975**, *46*, 326−342.
(126) Eaton, S.; Bartlett, K.; Pourfarzam, M. Mammalian mitochondrial beta-oxidation. *Biochem. J.* **1996**, *320*, 345−357.
(127) Green, D. W.; Grover, G. J. The IF(1) inhibitor protein of the mitochondrial F(1)F(0)-ATPase. *Biochim. Biophys. Acta* **2000**, *1458*, 343−355.
(128) Feliu, J. E.; Hue, L.; Hers, H. G. Hormonal control of pyruvate kinase activity and of gluconeogenesis in isolated hepatocytes. *Proc. Natl. Acad. Sci. U.S.A.* **1976**, *73*, 2762−2766.
(129) Argaud, D.; Roth, H.; Wiernsperger, N.; Leverve, X. M. Metformin decreases gluconeogenesis by enhancing the pyruvate kinase flux in isolated rat hepatocytes. *Eur. J. Biochem.* **1993**, *213*, 1341−1348.
(130) Moreno, F. J.; Benito, M.; Sanchez-Medina, F.; Medina, J. M.; Mayor, F. Pyruvate kinase activity and gluconeogenesis in rat liver after glycogen depletion with nicotinic acid. *Mol. Cell. Biochem.* **1976**, *13*, 89−93.
(131) Tielens, A. G.; Rotte, C.; van Hellemond, J. J.; Martin, W. Mitochondria as we don't know them. *Trends Biochem. Sci.* **2002**, *27*, 564−572.
(132) van Hellemond, J. J.; van der Klei, A.; van Weelden, S. W.; Tielens, A. G. Biochemical and evolutionary aspects of anaerobically functioning mitochondria. *Philos. Trans. R. Soc., B* **2003**, *358*, 205−213 discussion 213−215.
(133) Takamiya, S.; Matsui, T.; Taka, H.; Murayama, K.; Matsuda, M.; Aoki, T. Free-living nematodes *Caenorhabditis elegans* possess in their mitochondria an additional rhodoquinone, an essential component of the eukaryotic fumarate reductase system. *Arch. Biochem. Biophys.* **1999**, *371*, 284−289.
(134) Rea, S.; Johnson, T. E. A metabolic model for life span determination in *Caenorhabditis elegans*. *Dev. Cell* **2003**, *5*, 197−203.
(135) Tielens, A. G. Energy generation in parasitic helminths. *Parasitol. Today* **1994**, *10*, 346−352.
(136) Meissner, B.; Boll, M.; Daniel, H.; Baumeister, R. Deletion of the intestinal peptide transporter affects insulin and TOR signaling in *Caenorhabditis elegans*. *J. Biol. Chem.* **2004**, *279*, 36739−36745.
(137) Hansen, M.; Hsu, A. L.; Dillin, A.; Kenyon, C. New genes tied to endocrine, metabolic, and dietary regulation of lifespan from a *Caenorhabditis elegans* genomic RNAi screen. *PLoS Genet.* **2005**, *1*, 119−128.

(138) Ching, T. T.; Paal, A. B.; Mehta, A.; Zhong, L.; Hsu, A. L. *drr-2* encodes an eIF4H that acts downstream of TOR in diet-restriction-induced longevity of *C. elegans*. *Aging Cell* **2010**, *9*, 545−557.
(139) Cabreiro, F.; Au, C.; Leung, K. Y.; Vergara-Irigaray, N.; Cocheme, H. M.; Noori, T.; Weinkove, D.; Schuster, E.; Greene, N. D.; Gems, D. Metformin retards aging in *C. elegans* by altering microbial folate and methionine metabolism. *Cell* **2013**, *153*, 228−239.
(140) Stout, G. J.; Stigter, E. C.; Essers, P. B.; Mulder, K. W.; Kolkman, A.; Snijders, D. S.; van den Broek, N. J.; Betist, M. C.; Korswagen, H. C.; Macinnes, A. W.; Brenkman, A. B. Insulin/IGF-1-mediated longevity is marked by reduced protein metabolism. *Mol. Syst. Biol.* **2013**, *9*, 679-1−679-13.
(141) Hansen, M.; Taubert, S.; Crawford, D.; Libina, N.; Lee, S. J.; Kenyon, C. Lifespan extension by conditions that inhibit translation in *Caenorhabditis elegans*. *Aging Cell* **2007**, *6*, 95−110.
(142) Syntichaki, P.; Troulinaki, K.; Tavernarakis, N. eIF4E function in somatic cells modulates ageing in *Caenorhabditis elegans*. *Nature* **2007**, *445*, 922−926.
(143) Pan, K. Z.; Palter, J. E.; Rogers, A. N.; Olsen, A.; Chen, D.; Lithgow, G. J.; Kapahi, P. Inhibition of mRNA translation extends lifespan in *Caenorhabditis elegans*. *Aging Cell* **2007**, *6*, 111−119.
(144) Lynch, C. J.; Fox, H. L.; Vary, T. C.; Jefferson, L. S.; Kimball, S. R. Regulation of amino acid-sensitive TOR signaling by leucine analogues in adipocytes. *J. Cell. Biochem.* **2000**, *77*, 234−251.
(145) Newgard, C. B.; An, J.; Bain, J. R.; Muehlbauer, M. J.; Stevens, R. D.; Lien, L. F.; Haqq, A. M.; Shah, S. H.; Arlotto, M.; Slentz, C. A.; Rochon, J.; Gallup, D.; Ilkayeva, O.; Wenner, B. R.; Yancy, W. S., Jr; Eisenson, H.; Musante, G.; Surwit, R. S.; Millington, D. S.; Butler, M. D.; Svetkey, L. P. A branched-chain amino acid-related metabolic signature that differentiates obese and lean humans and contributes to insulin resistance. *Cell Metab.* **2009**, *9*, 311−326.
(146) Newgard, C. B. Interplay between lipids and branched-chain amino acids in development of insulin resistance. *Cell Metab.* **2012**, *15*, 606−614.
(147) Fisher, A. L.; Lithgow, G. J. The nuclear hormone receptor DAF-12 has opposing effects on *Caenorhabditis elegans* lifespan and regulates genes repressed in multiple long-lived worms. *Aging Cell* **2006**, *5*, 127−138.
(148) Schulz, T. J.; Zarse, K.; Voigt, A.; Urban, N.; Birringer, M.; Ristow, M. Glucose restriction extends *Caenorhabditis elegans* life span by inducing mitochondrial respiration and increasing oxidative stress. *Cell Metab.* **2007**, *6*, 280−293.
(149) Williams, D. S.; Cash, A.; Hamadani, L.; Diemer, T. Oxaloacetate supplementation increases lifespan in *Caenorhabditis elegans* through an AMPK/FOXO-dependent pathway. *Aging Cell* **2009**, *8*, 765−768.
(150) Hamilton, B.; Dong, Y.; Shindo, M.; Liu, W.; Odell, I.; Ruvkun, G.; Lee, S. S. A systematic RNAi screen for longevity genes in *C. elegans*. *Genes Dev.* **2005**, *19*, 1544−1555.
(151) Wong, A.; Boutis, P.; Hekimi, S. Mutations in the *clk-1* gene of *Caenorhabditis elegans* affect developmental and behavioral timing. *Genetics* **1995**, *139*, 1247−1259.
(152) Feng, J.; Bussiere, F.; Hekimi, S. Mitochondrial electron transport is a key determinant of life span in *Caenorhabditis elegans*. *Dev. Cell* **2001**, *1*, 633−644.
(153) Dillin, A.; Crawford, D. K.; Kenyon, C. Timing requirements for insulin/IGF-1 signaling in *C. elegans*. *Science* **2002**, *298*, 830−834.
(154) Murphy, C. T.; Lee, S.-J.; Kenyon, C. Tissue entrainment by feedback regulation of insulin gene expression in the endoderm of *Caenorhabditis elegans*. *Proc. Natl. Acad. Sci. U.S.A.* **2007**, *104*, 19046−19050.
(155) Aitlhadj, L.; Sturzenbaum, S. R. The use of FUdR can cause prolonged longevity in mutant nematodes. *Mech. Ageing Dev.* **2010**, *131*, 364−365.
(156) Van Raamsdonk, J. M.; Hekimi, S. FUdR causes a twofold increase in the lifespan of the mitochondrial mutant gas-1. *Mech. Ageing Dev.* **2011**, *132*, 519−521.
(157) Davies, S. K.; Leroi, A. M.; Bundy, J. G. Fluorodeoxyuridine affects the identification of metabolic responses to *daf-2* status in *Caenorhabditis elegans*. *Mech. Ageing Dev.* **2012**, *133*, 46−49.